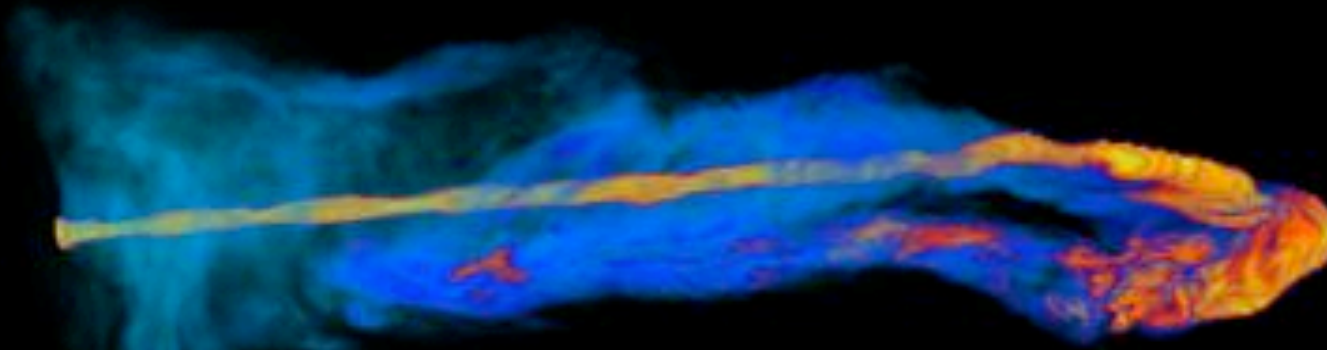


RELATIVISTIC JETS IN ASTROPHYSICS

Computer simulations and experimental validation



Attilio Ferrari

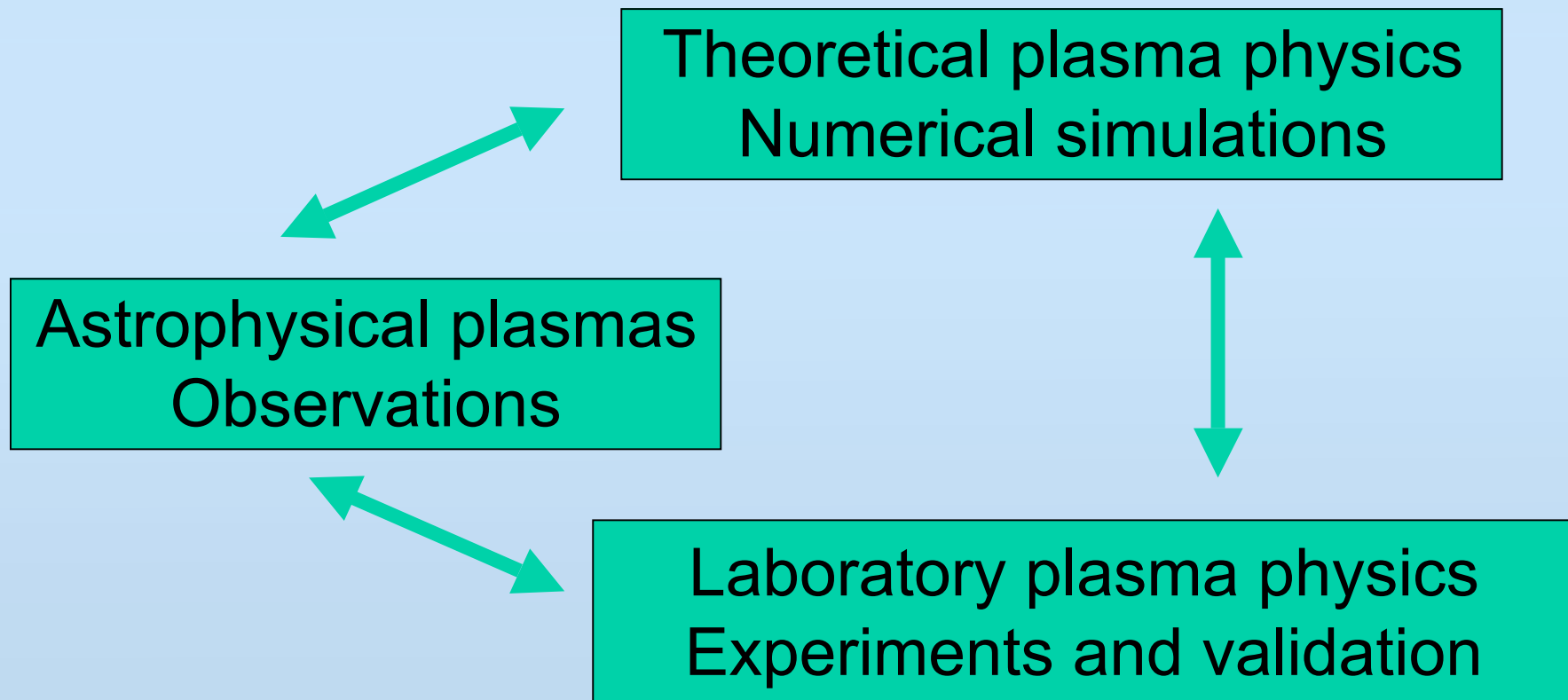
CIFS Consorzio Interuniversitario per la Fisica Spaziale
Dipartimento di Fisica Generale, Università di Torino
INAF Osservatorio Astronomico di Torino
INFN, Sezione di Torino



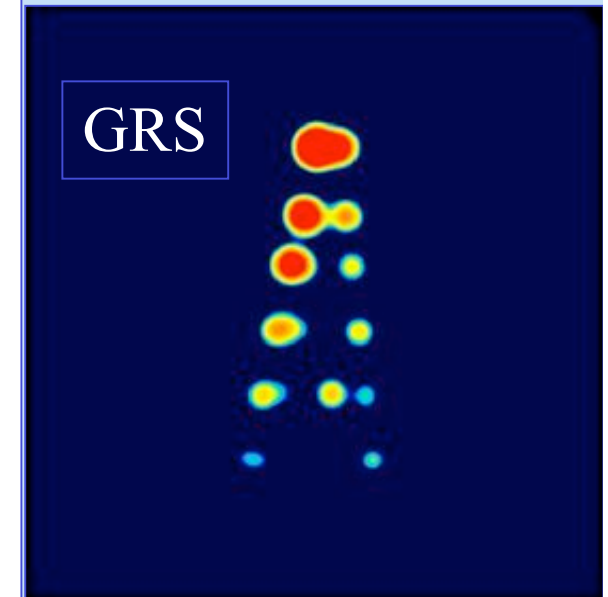
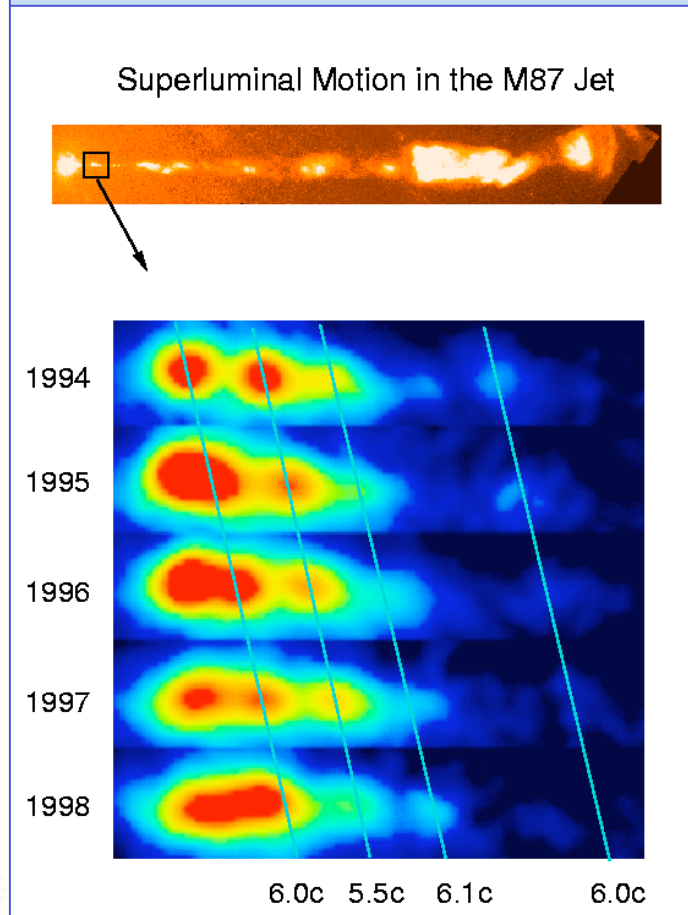
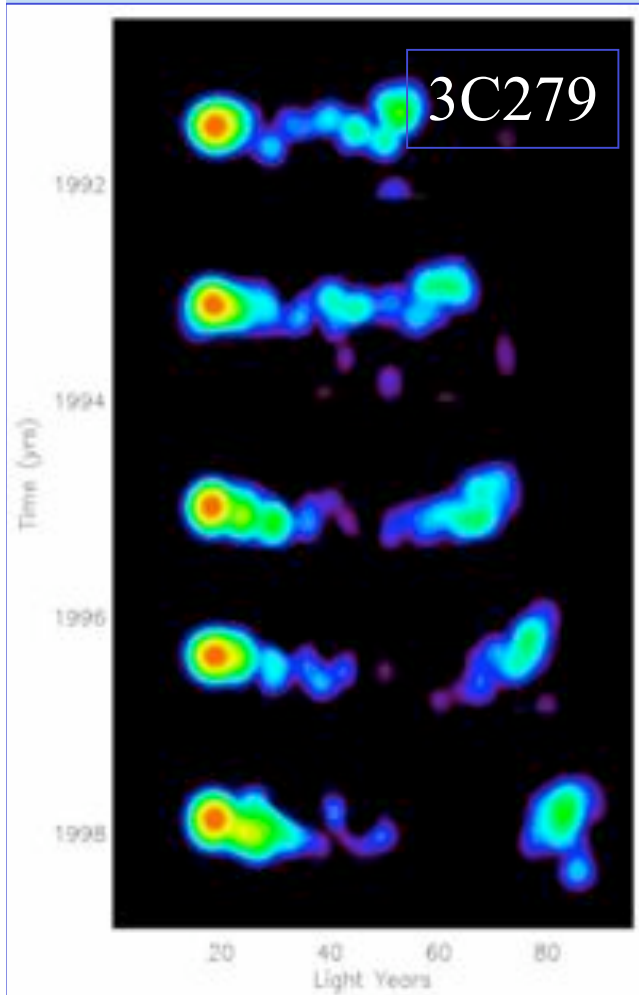
Plasmas in Astrophysics and in the Laboratory - The Ignitor Challenge
Moscow, 20 - 21 June 2011



Highly nonlinear (relativistic) physics
Huge extension of physical parameters
Scalability



Astrophysical Evidence of Relativistic Jets



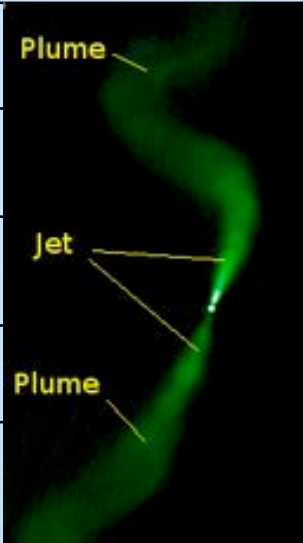
Superluminal motions & Doppler boosting jet/counter-jet
(Cohen et al. 1971, Biretta et al. 1999, Mirabel et al 1992)

Jets and VHE Sources Variabilities

- Blazars, energetics (Oke & Gunn 1974)
- VHE emission and rapid variabilities correlated with X rays and radio emission
 - Mkn 421 (AGILE, Donnarumma et al. 2009)
 - M87 (FERMI, Acciari et al. 2009)
- GRBs, energetics and spectra (Klebesadel et al. 1973)
- Doppler boosting in relativistic jets moving towards the observer
- Light jets with relativistic spine and slower sheath layer
 - Spine produces synchrotron optical and X-ray photons, that are boosted to GeV and TeV gamma rays by inverse Compton in the sheath (e.g. Chiaberge et al. 2000, Tavecchio & Ghisellini 2008)
 - Radio emission from extended (expanding) cocoon

Relativistic radio jets

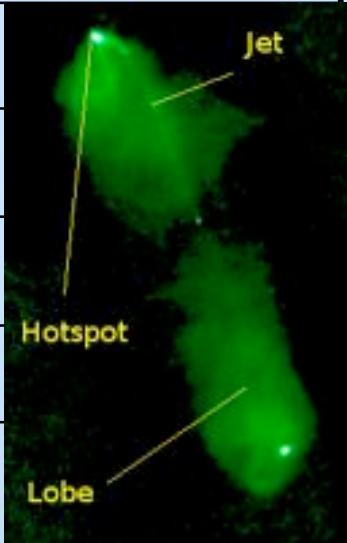
	FR I	FR II
0.1 pc	$\gamma \approx 10-20$	$\gamma \approx 20-30$
1 pc	$\gamma \approx 3-20$	
100 pc	$\gamma \approx 5$	
1 kpc	$\gamma \approx 2$	$\gamma > 10$
10 kpc	$\gamma \approx .2$	$\gamma > 4$



Plume

Jet

Plume



Jet

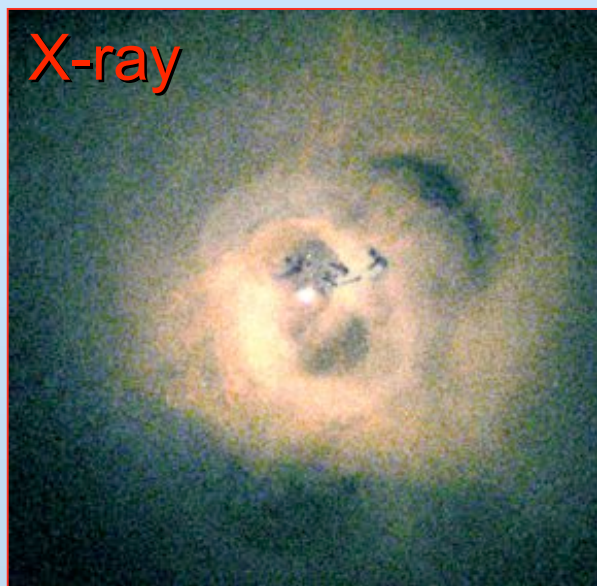
Hotspot

Lobe

(Giovannini et al. 2005, Laing et al. 2008)

Jet Dissipation

- Clusters and groups of galaxies emit X-rays
- Thermal bremsstrahlung from hot (0.5 keV up to 10 keV) gas confined in potential well: hot Intra-Cluster Medium (ICM)
- Heating mechanism?
- Evidence that AGN jets affect the ICM

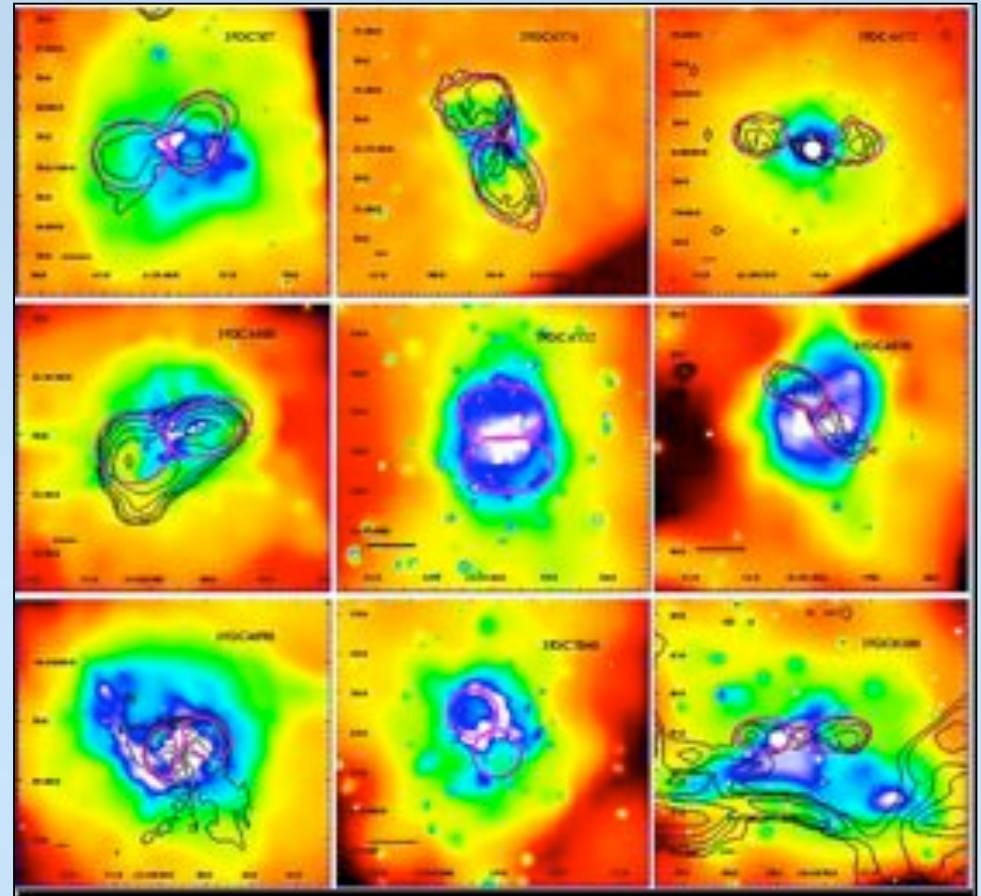
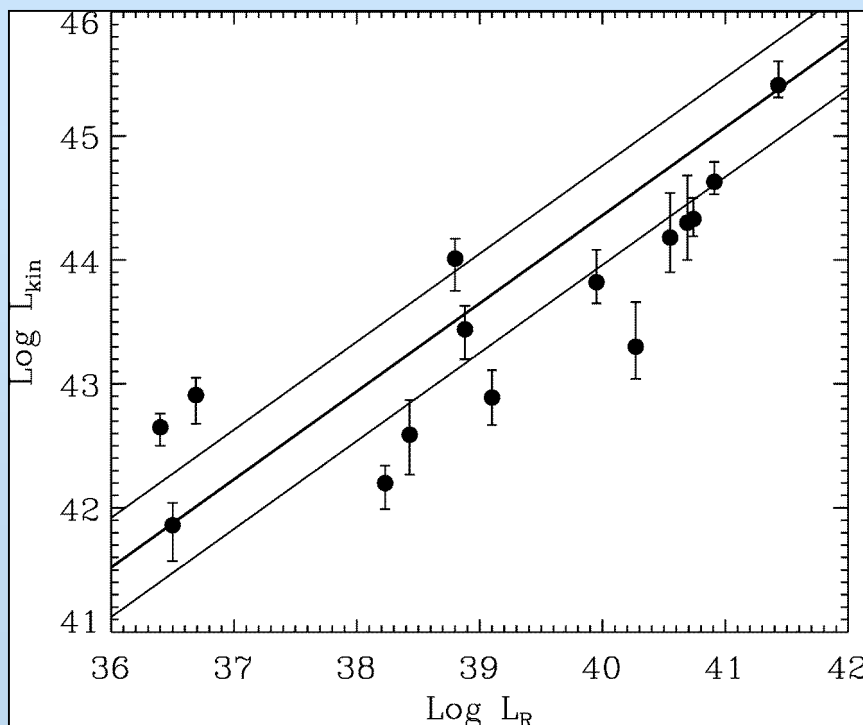


- X-ray cavities corresponding to radio lobes
- Shells surrounding the cavities
- Shell temperature lower than the surrounding medium: weak shocks

Fabian et al. (2003, 2005)
Perseus cluster (CHANDRA)

Work done to produce cavities (Allen et al. 2006, Heinz et al. 2007):

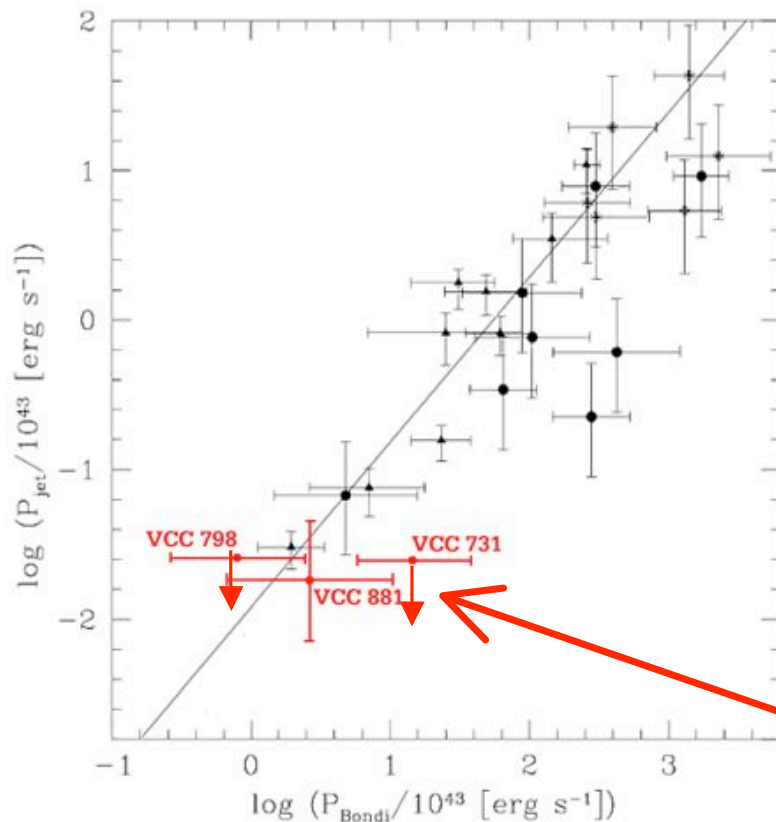
$$W = \frac{\gamma}{\gamma - 1} PV \rightarrow L_{kin} = \frac{W}{t_{age}}$$



$$L_{kin} = 10^{37} \left(\frac{L_{\nu, radio\ core}}{7 \times 10^{22}} \right)^{12/17} W$$

Accretion and jets

Correlation between the accretion onto BH and the jet kinetic power (Allen et al. 2006, Heinz et al. 2007, Balmaverde et al. 2008)

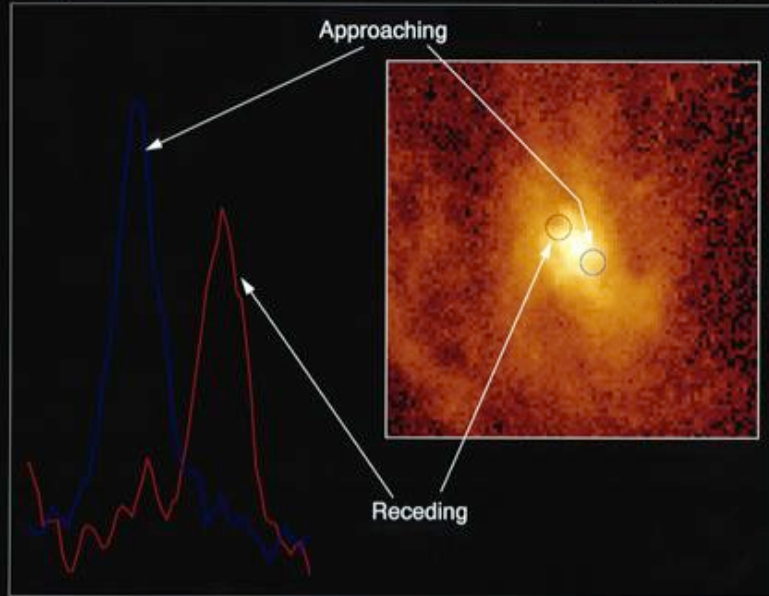


$$1) P_B = \dot{M}_B c^2, \quad \dot{M}_B = \frac{\pi G^2 \rho_B M_{BH}^2}{c_s^3}$$

$$2) P_j = 8.6 \times 10^{22} L_{\nu, radio\ core}^{12/17} \text{ erg s}^{-1}, \alpha_\nu = 0$$

Radio quiet

Spectrum of Gas Disk in Active Galaxy M87

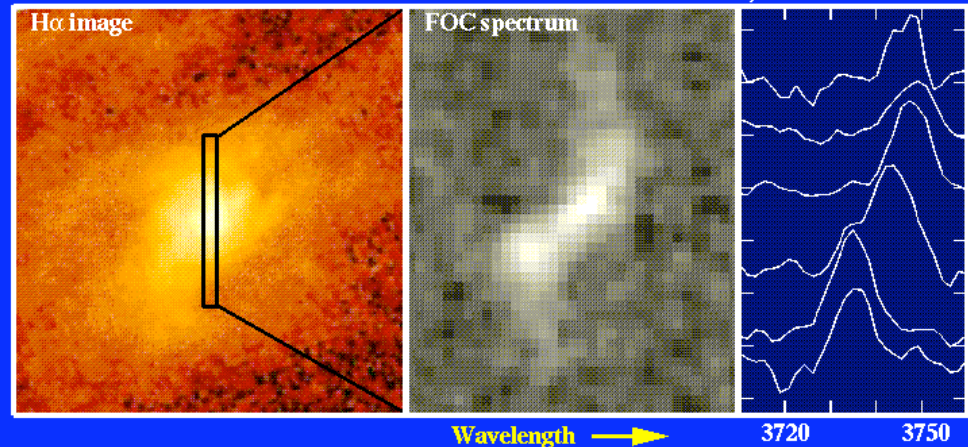
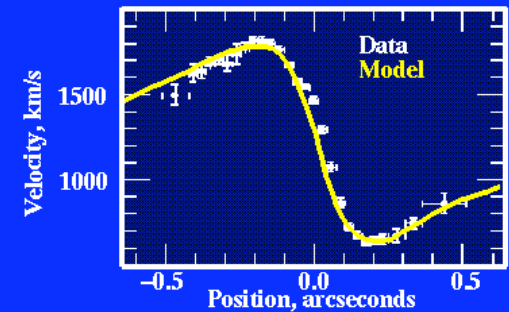


Hubble Space Telescope · Faint Object Spectrograph

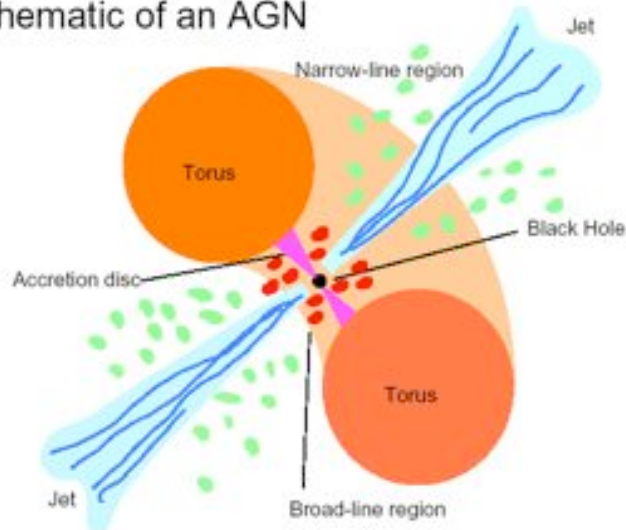
High resolution photometry and spectroscopy from HST
Compact rotating SMBH

Velocity Profiles in the M87 Core

Model: central mass 3.2×10^9 solar masses



Schematic of an AGN



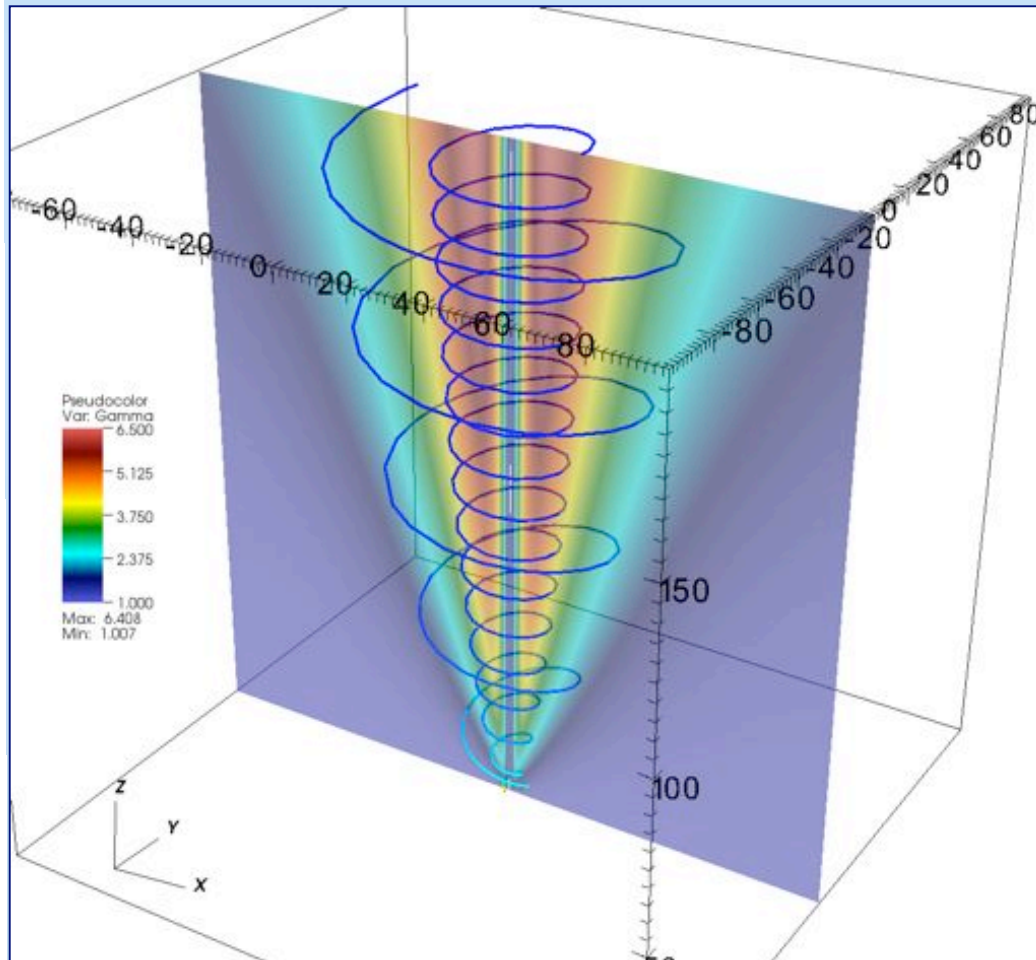
The disk-jet paradigm

RMHD Jet Launching

- Two energy reservoirs:

Keplerian disk accretion ($\Omega = \Omega_{\text{Keplerian}}$)

Kerr black hole rapid rotation ($\Omega_H = ac/2R_H$ $J_H = aGM^2/c$ $-1 < a < 1$)

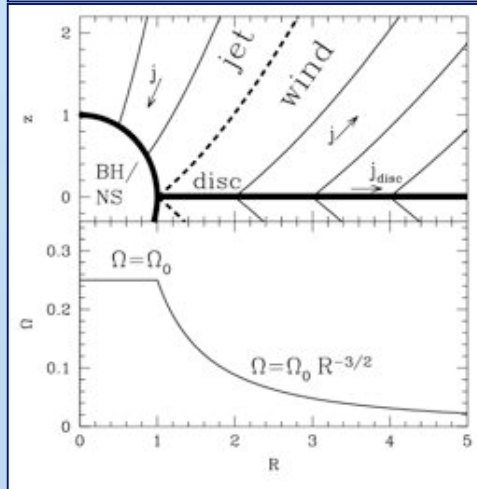
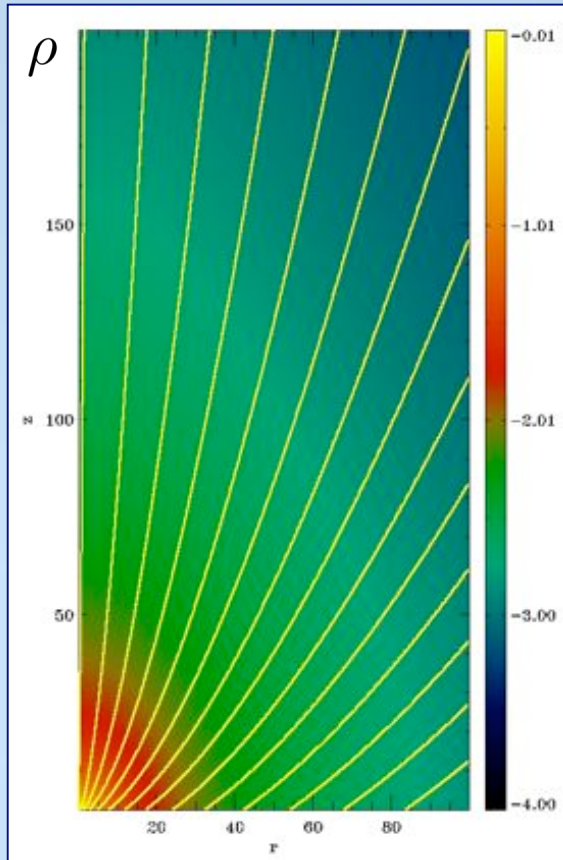


- Twisted magnetic field extracts rotational energy at a rate \dot{E} mainly in the form of Poynting flux
- Mass outflow rate \dot{M}
- The specific energy $\mu = \dot{E}/\dot{M}c^2$ is the maximum possible Lorentz factor of the outflow
- Which is the asymptotic Lorentz factor γ_∞ and the acceleration efficiency ?

Acceleration efficiency

- Analytic solutions (e.g. review Königl 2010) $\longrightarrow \mu = \dot{E}/\dot{M}c^2$
- Michel (1969): acceleration along a monopolar field essentially ends at the fast-magnetosonic surface with $\gamma_\infty \simeq \mu^{1/3} \ll \mu$
 \longrightarrow inefficient acceleration
- In a non-relativistic flow the kinetic energy at the fast surface is already 1/3 of the total energy available $E_{kin,FM} \simeq E_{tot}/3$
 \longrightarrow acceleration is more efficient in the classical regime !
- Both analytical self-similar models (Li, Chiueh, Begelman 1992, Vlahakis & Königl 2003, 2004) and numerical simulations (Komissarov et al. 2007, 2009, Tchekhovskoy et al. 2009) suggest that the acceleration process can be much more efficient, with $\gamma_\infty \simeq \mu/2$ or even higher

Numerical Simulations



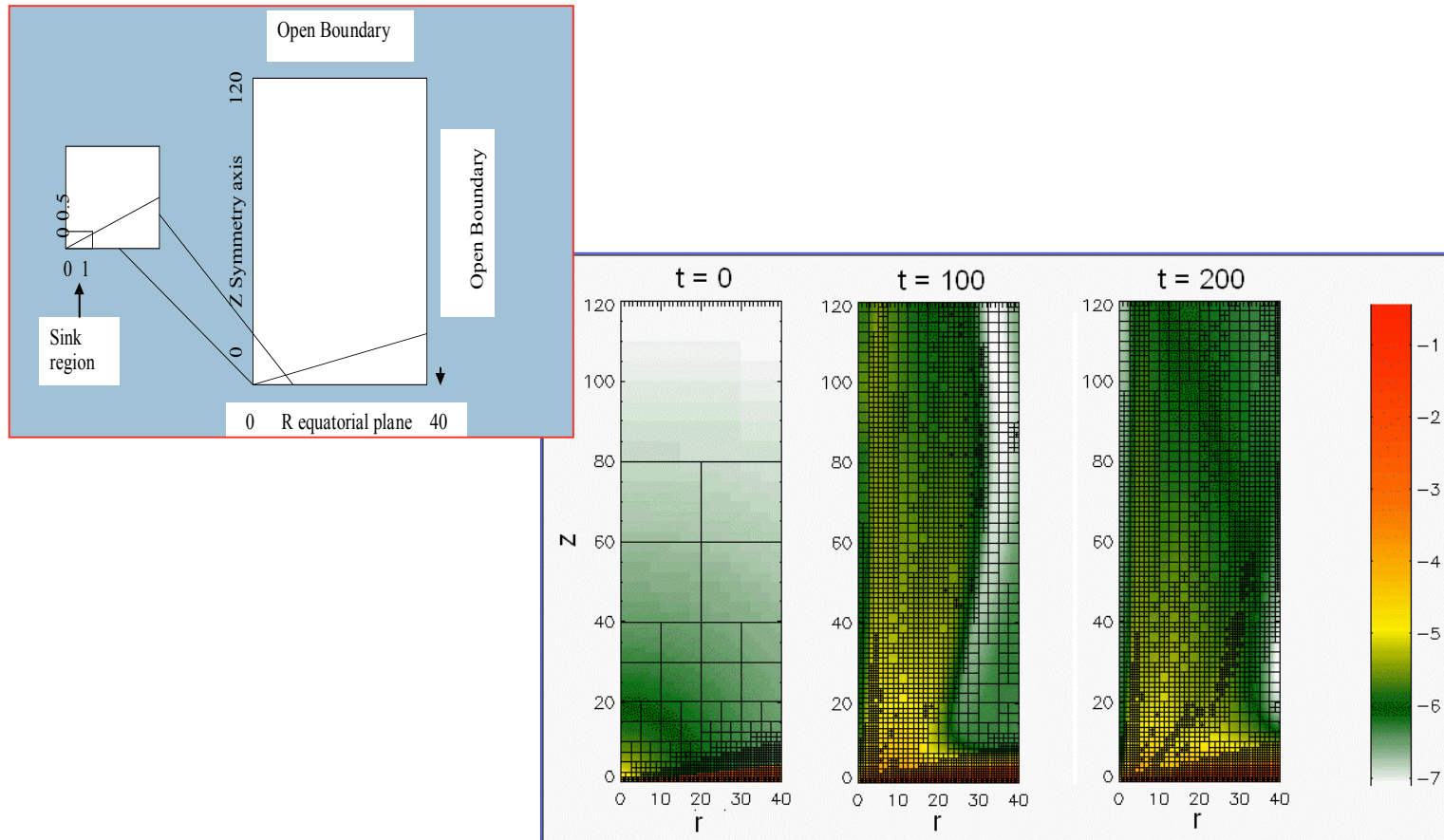
- Special relativistic MHD: gravitational effects neglected, focus on large scale acceleration
- Initial and boundary conditions:
 - rotating boundary
[solid rotator (BH/NS) + Keplerian disk]
 - purely poloidal current-free magnetic field
 $B_p \propto r^{-5/4}$ (Blandford & Payne 1982)
 - plasma injected with poloidal speed $\gamma_{inj} \simeq 1$
- Simulation evolved up to stationary state
- Steady state: RMHD axisymmetric invariants

Specific energy: $\mu = \gamma - \frac{r\Omega B_\phi}{\Psi} = \text{kinetic} + \text{Poynting}$



Acceleration = transfer of Poynting to kinetic flux

2.5 D MHD
Codes
FLASH2.5
& PLUTO
with AMR
7 levels of refinement



Starting from “quasi-Keplerian” disk in equilibrium with gravity, thermal pressure gradient and Lorentz force \rightarrow search for stationary states

Alpha prescription for momentum transport

Disk parameters: $\mu = B^2/2P = 0.6$

$\varepsilon = c_s / V_K = 0.1$

$H = \varepsilon r$

$\eta_m = \alpha_m v_A H \exp[-2(z/H)^2]$

Cases: a) $\alpha_m = 0.1$ $\chi_m = 1$ poloidal/toroidal

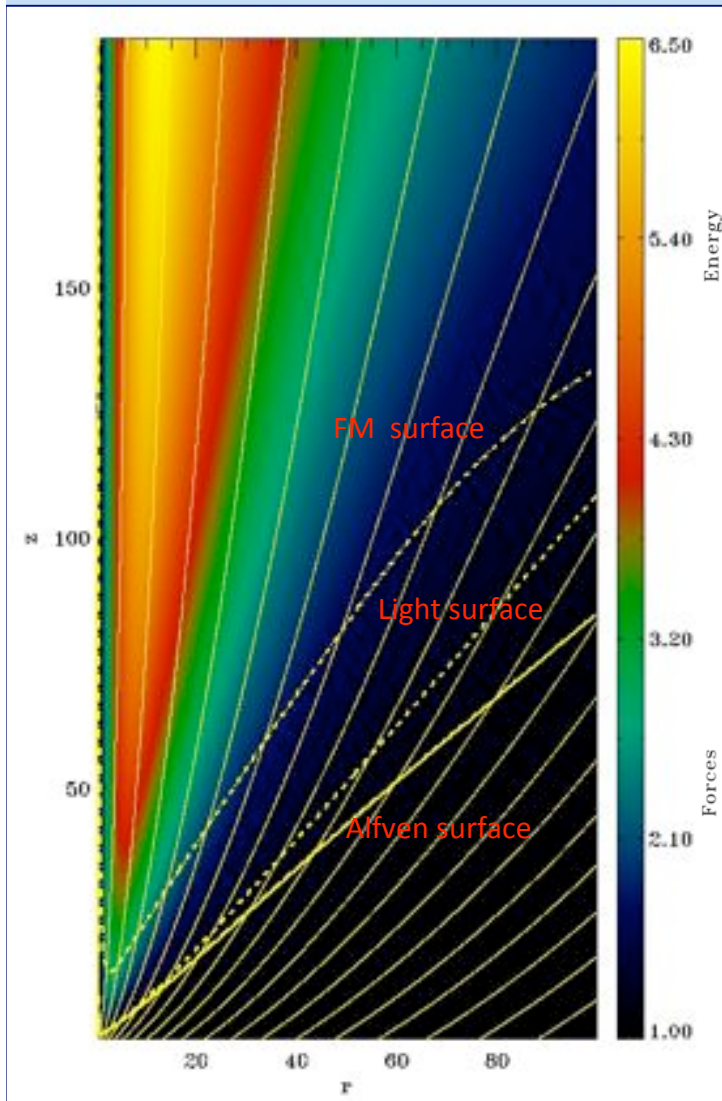
b) $\alpha_m = 1$ $\chi_m = 1$

c) $\alpha_m = 1$ $\chi_m = 3$

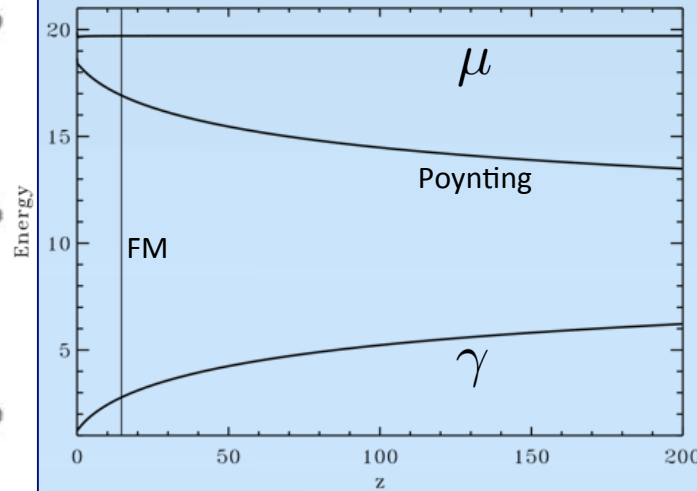
d) $\alpha_m = 0.1$ $\chi_m = 1$ low resolution

Jet Acceleration

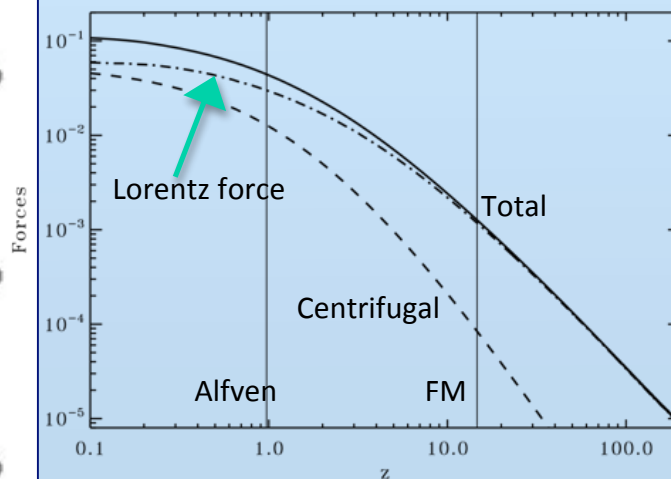
Lorentz Gamma



Along a magnetic surface with $r_0 = 1$

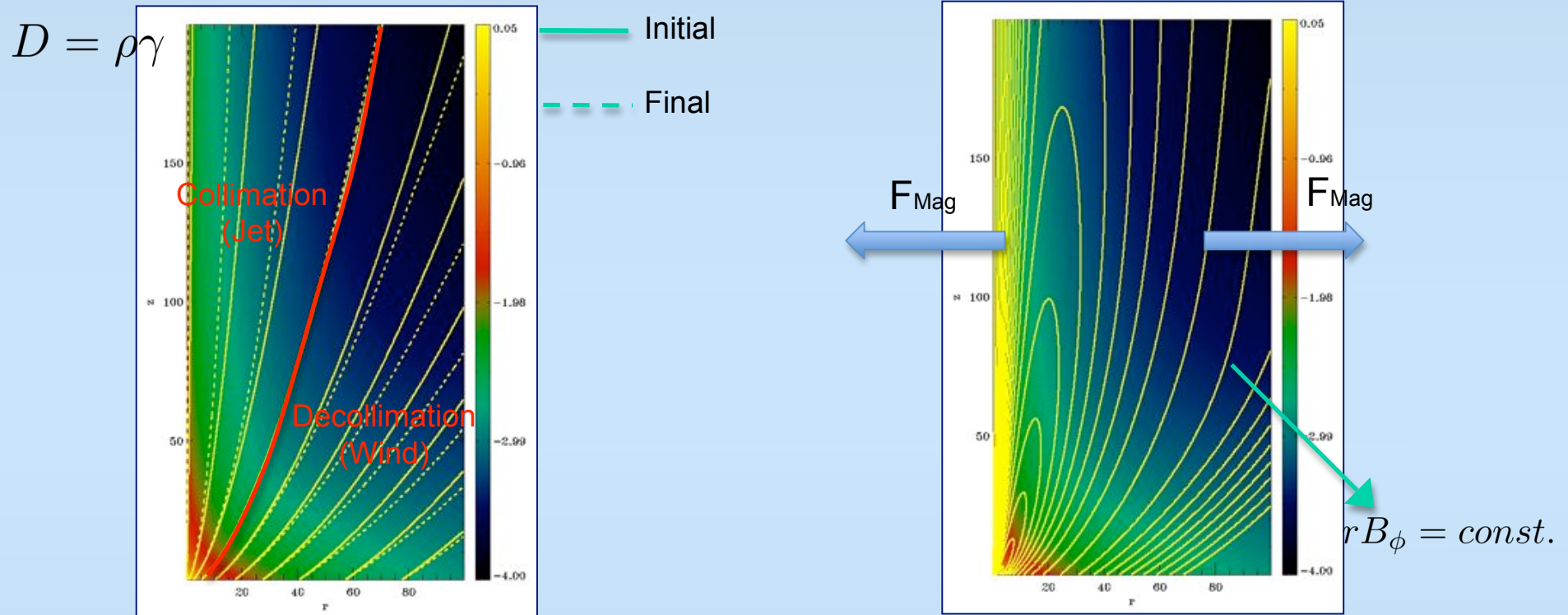


- Flow accelerates even beyond FM surface up to $\gamma \sim 6$ with an efficiency $\gamma \sim 0.3\mu$
- Flow is still accelerating! (need larger simulations)



- Flow accelerated by Lorentz forces (B_ϕ pressure) and centrifugal effects
- Beyond FM surface magnetic pressure drives the flow (magnetic nozzle, Li et al. 1992)

Jets, winds and (de)collimation



- The magnetic force associated with the toroidal field (perpendicular to the $rB_\phi = const.$ isosurfaces) tends to collimate the inner field lines and to decollimate the outer ones, creating a configuration favorable for efficient acceleration.
- The structure suggests a fast jet (collimated) – slower wind (decollimated) configuration.
- In the relativistic regime, the electric force is comparable to the magnetic but with opposite sign: differential collimation and acceleration are still possible but on very long spatial scales.

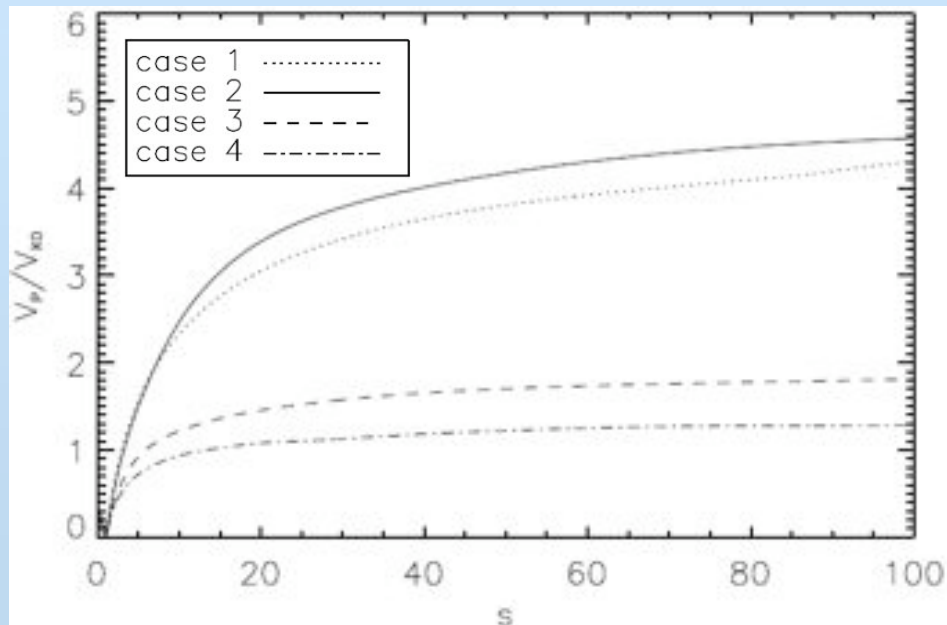
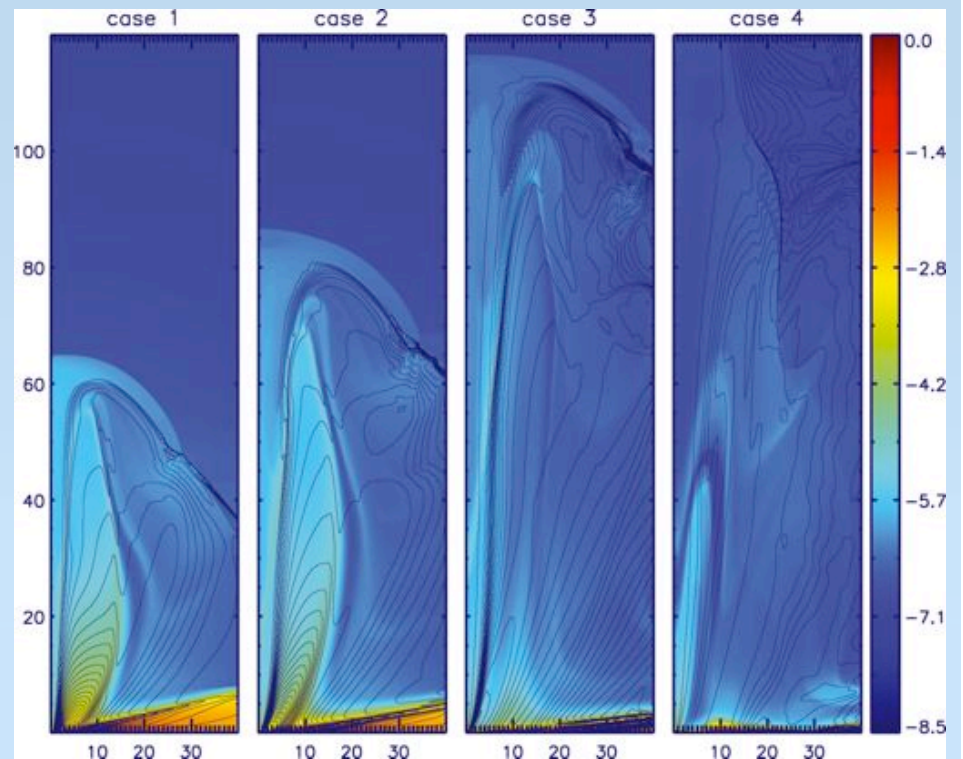
- *Focus: magnetization*
- Resistive 2.5D MHD simulations of jet launching:

$$\beta = 2P / B^2$$

- From weak (case 1, 2) to strong magnetic fields (case 3, 4)

$$1/3 \leq \beta \leq 10.0$$

Tzeferacos et al. MNRAS 2009

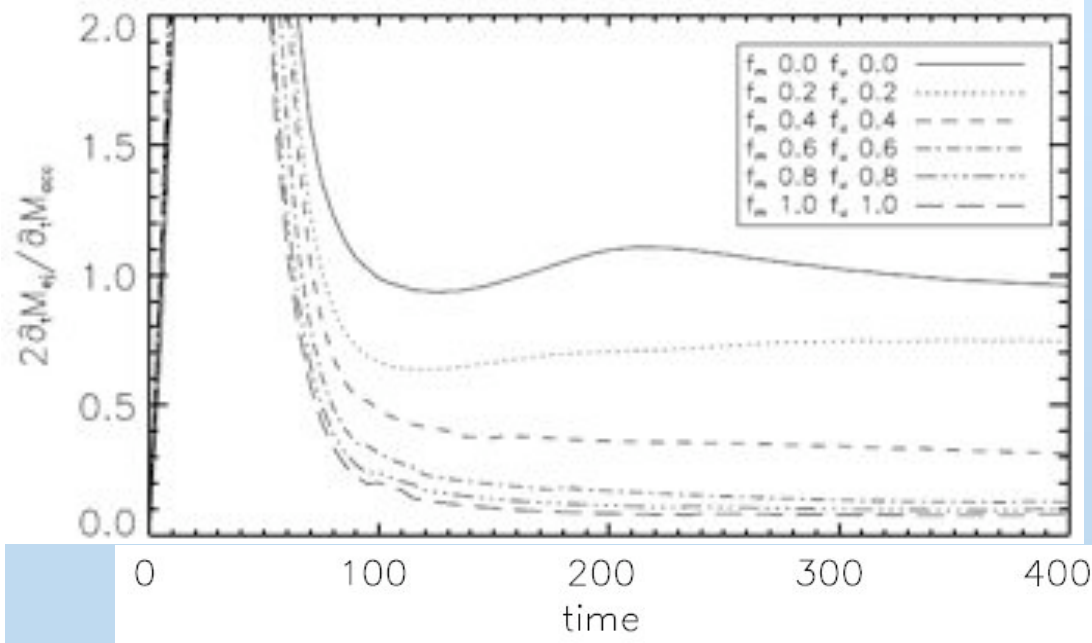
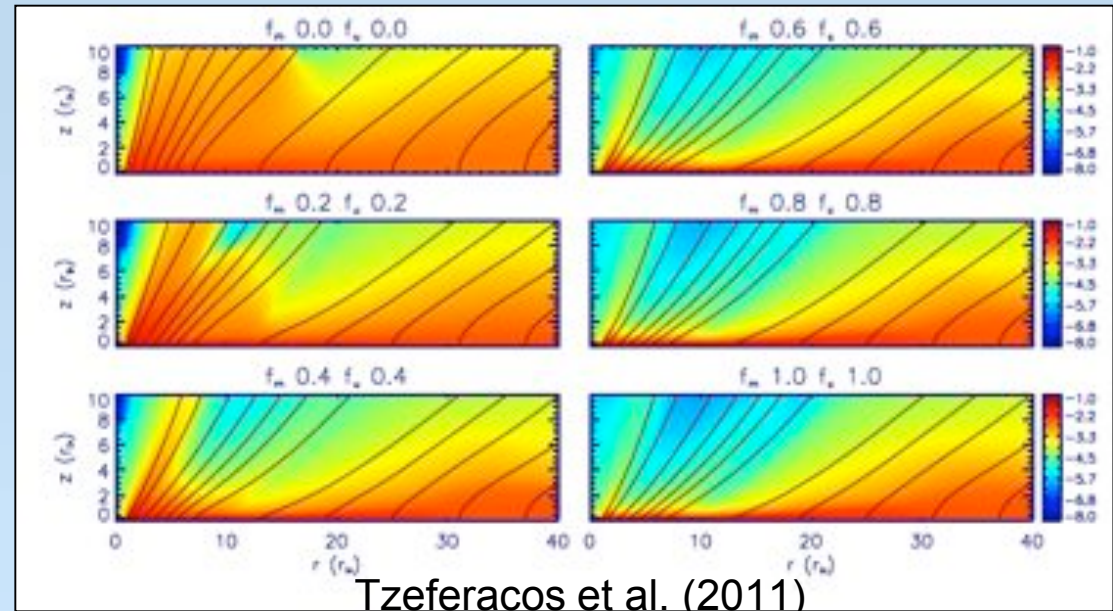


- Self-consistent jet ejection from accretion disc
- Super Alfvénic, super fast magneto-sonic outflows
- *Steady state solutions obtained only above equipartition plasma β (case 1,2)*

- Focus: entropy generation
due to viscous and Ohmic heating

- Viscous and resistive 2.5D MHD simulations of jet launching

- α prescription for viscosity and resistivity, with magnetic Prandtl number: $P_m = \eta_u / \eta_m \sim 1$



- Strong correlation between disk heating effects and mass loading.

- Efficient acceleration and stationarity is found for mildly warm and cold cases, comparable to slow radio-galaxies and YSO jets

Challenging the alpha prescription

Momentum transport
Viscosity of α -disks:

$$\nu = \alpha c_s H e^{-2\left(\frac{z}{H}\right)^2}$$

Alpha and disk physical
parameters?

“Measured” values of α

Numerical simulations of MRI <i>varies with large-scale field, dissipation terms</i>	10^{-3} - 10^{-1}
Protostellar disks <i>based on disk masses, temperatures, accretion rates, and lifetimes</i>	10^{-2} - 10^{-3}
Cataclysmic variables <i>based on models of “dwarf nova” outbursts</i>	10^{-3} - 10^0
AGN <i>direct observational constraints are few to none</i>	?

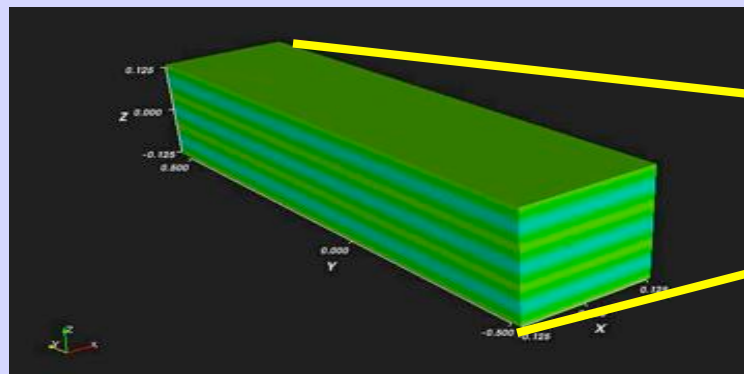
Numerical simulations of MRI
Effects of the numerics?

3D high-resolution simulation
in shearing box approximation
(Sano & Inutsuka 2001, Mignone et al 2009)
In a cartesian frame of reference corotating
with the disk

The channel solution, intermittent states,
transition to turbulence, calculation of
Maxwell stresses, aspect ratio dependence

Dynamo

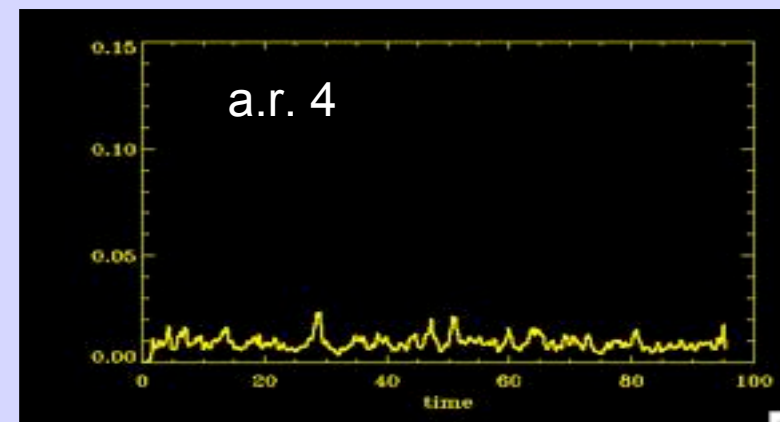
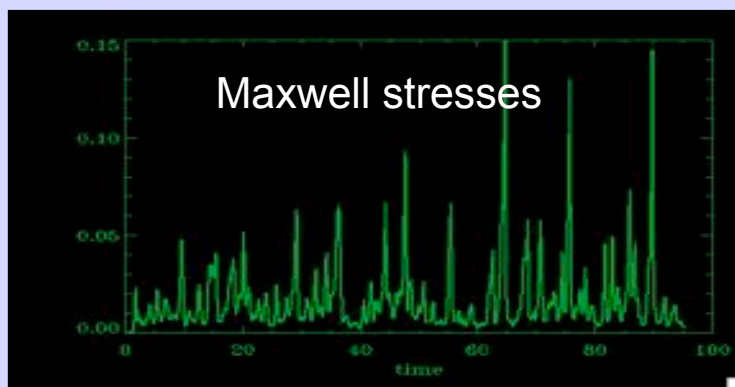
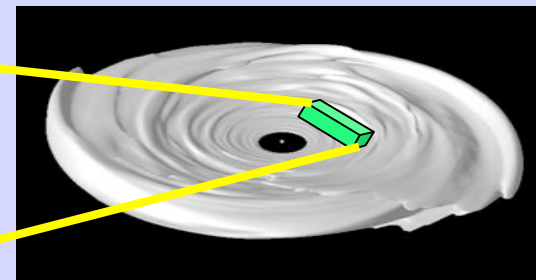
Maxwell stresses and alpha



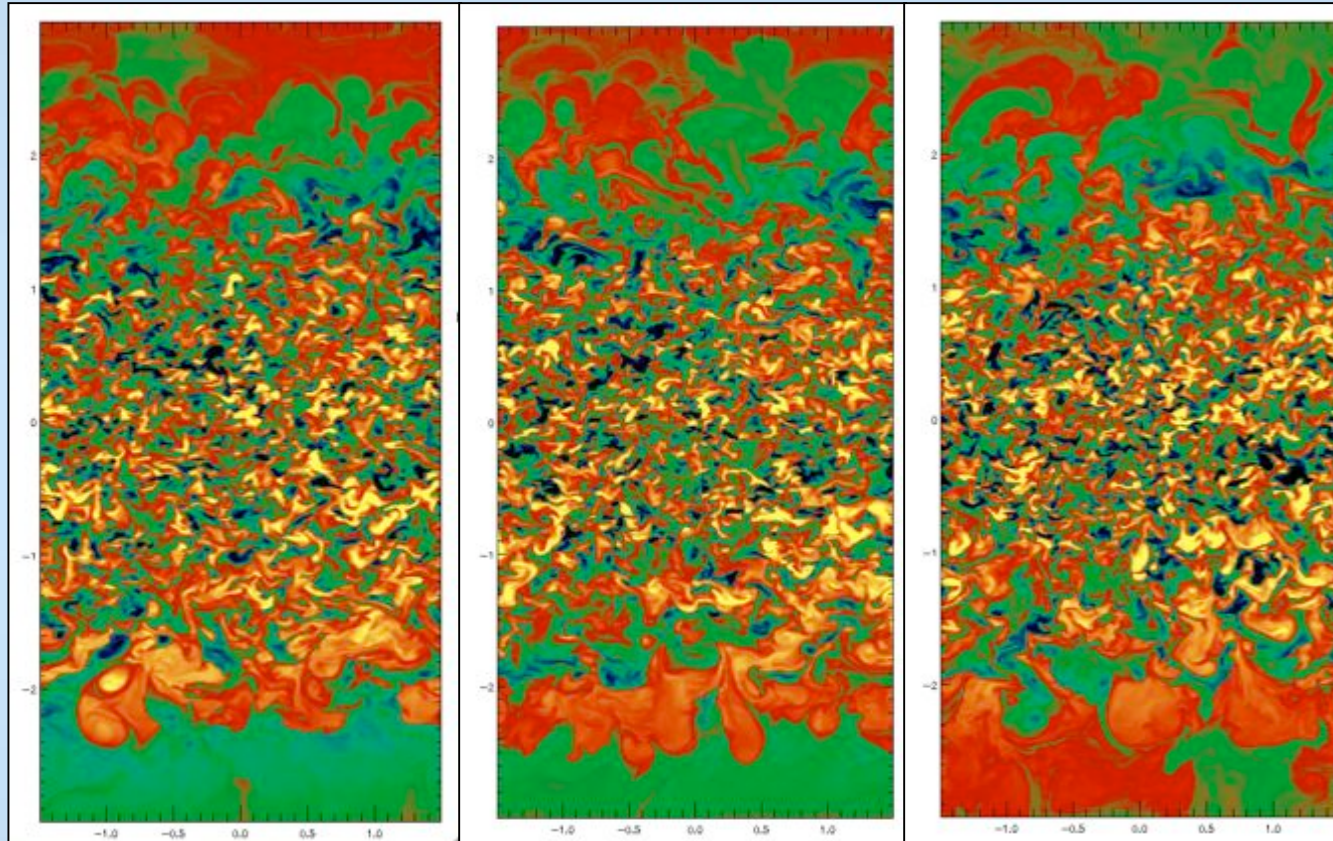
Unstratified shearing boxes have been
shown to suffer from many problems
(Fromang et al. 2007, Regev & Umhuran 2008,
Bodo et al. 2008, 2010)

In particular with zero mean
field the transport becomes
negligible at high Reynolds
numbers: artifact of shearing box

Towards global simulations



Preliminary results from simulations in which gravitational stratification is included
Still shearing box conditions in the radial direction. First step towards global simulations.



Azimuthal
Component
of the magnetic
field.
x-z cut

Domain size $3H \times 4H \times 6H$ (H density scale height). 200 points per scale height.

Turbulent region in the denser region in the middle

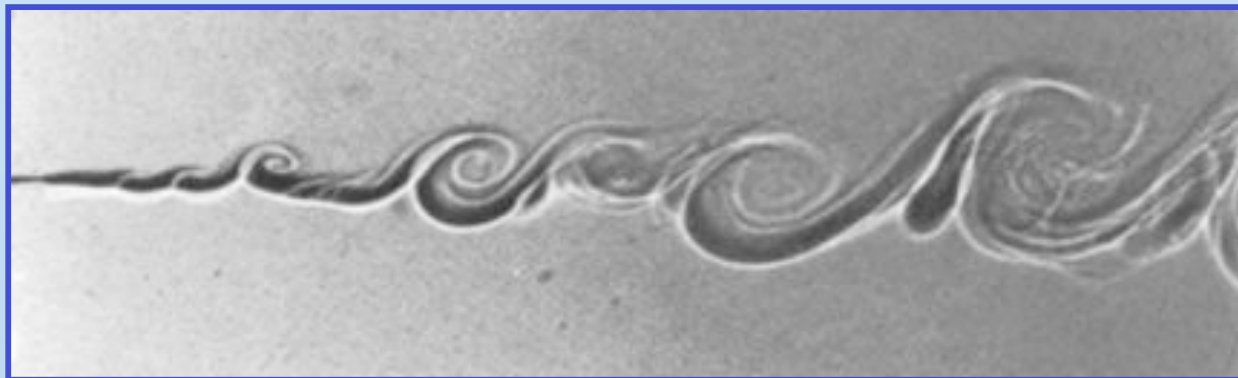
Interesting point: periodic formation of highly magnetized regions in the upper and lower regions (magnetized coroneae)

Relativistic Jet Propagation

- Are jets stable ?
- Do they dissipate magnetic flux ?
- Intrinsic/external instabilities
- How do jets decelerate without decollimating ?
- Mass entrainment from the ambient medium across an unstable boundary layer
 - *“internal”* entrainment: diffusion of mass lost from stars within the jet volume (Komissarov 1994)
 - *“external”* entrainment: ingestion of ambient gas from the surrounding IGM via a turbulent unstable boundary layer (Begelman 1982; De Young 1996)
- Connecting morphologies with dynamics
- Instabilities and turbulent particle acceleration

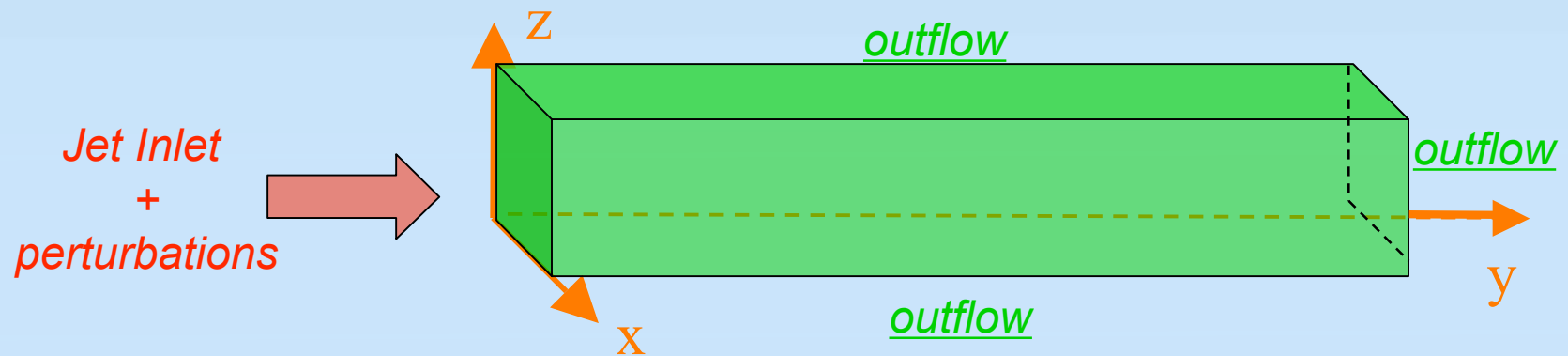
Interaction with external medium

- Shear instabilities in supersonic flows (Brown & Roshko 1974)
- Relativistic Kelvin-Helmholtz instabilities in astrophysical jets (Ferrari et al. 1978, Hardee 1987, etc.)
- Stabilized by extended shear layers and longitudinal magnetic fields; nonlinear saturation effects (Benford et al. 1980)



3D Relativistic Hydro Jets

- ❑ Solve the full set of inviscid relativistic hydro equations in 3D:
- ❑ Computational domain:



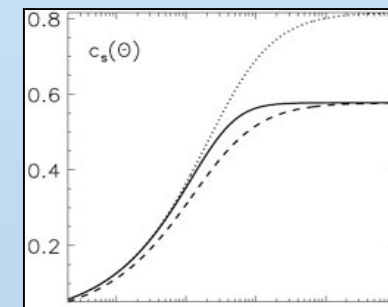
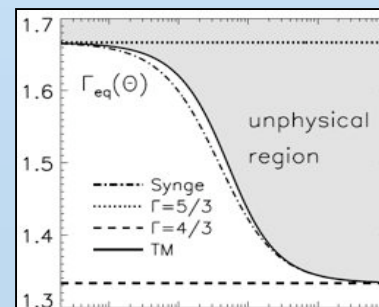
- ❑ Cartesian coordinates, homogeneous external medium, pressure matched jet
- ❑ Perturbations at the jet inlet: pinching, helical, fluting

$$\gamma_b = \gamma_b (1 + \varepsilon) \Rightarrow \varepsilon \approx 0.05$$

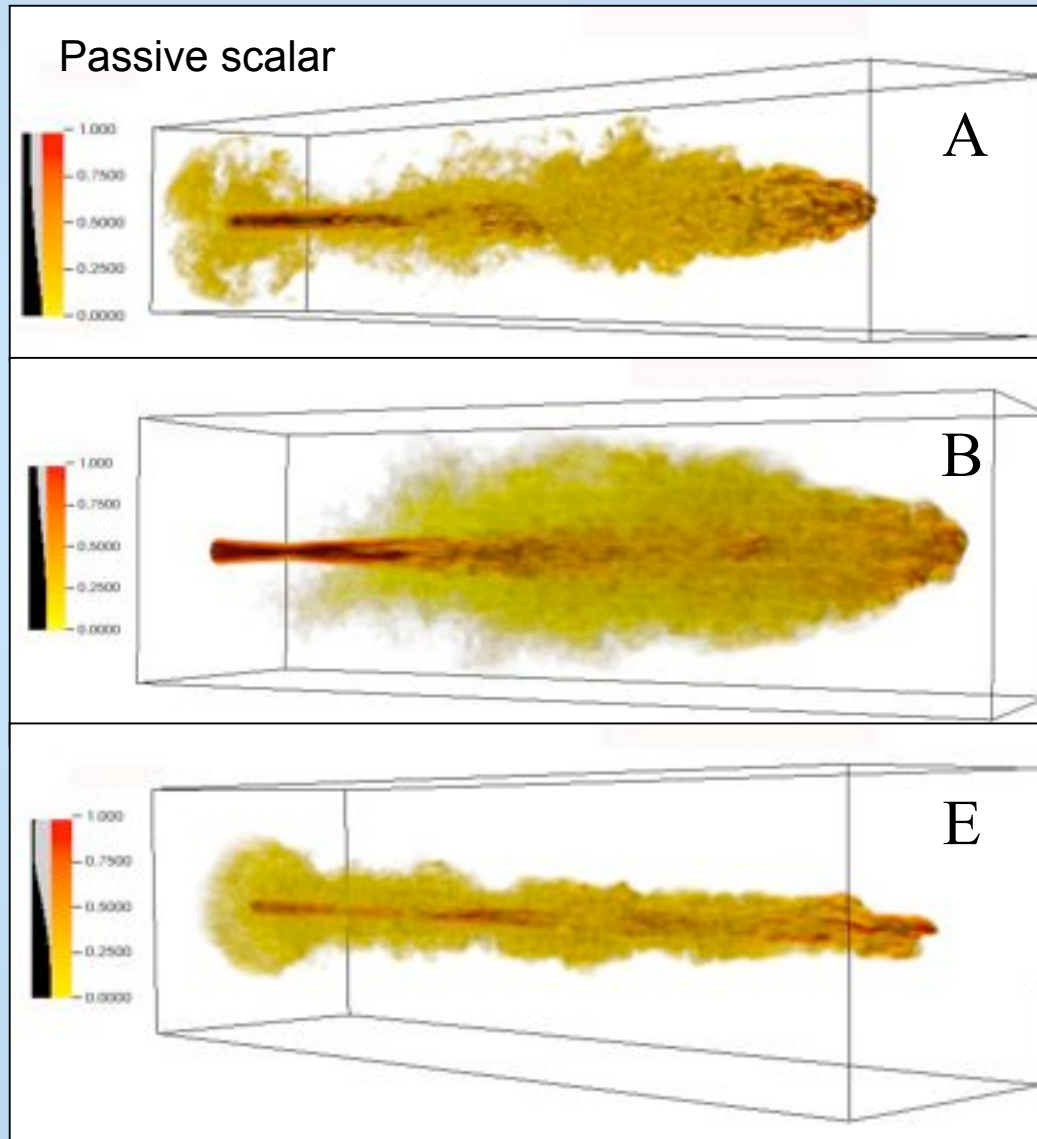
- ❑ Relativistic Mach number

$$M_r = \gamma_b v_b / \gamma_s v_s$$

- ❑ Sygne EoS



Mixing by Shear Instabilities



$$\gamma = 10, M = 3, \eta = 10^2$$

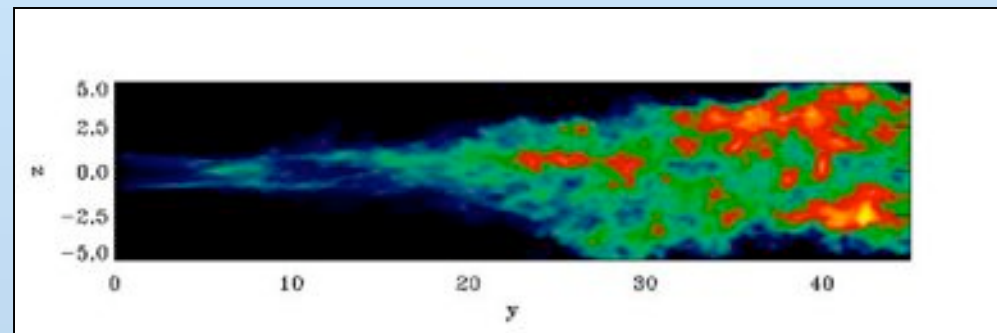
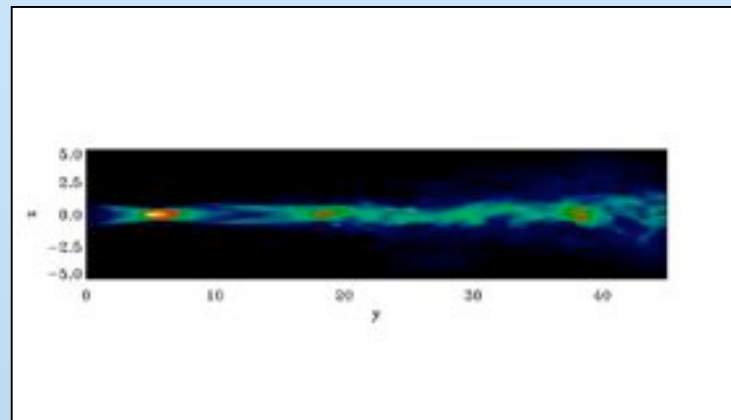
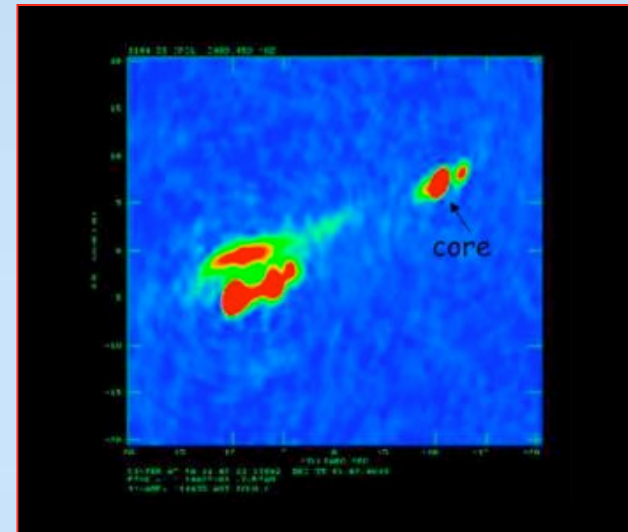
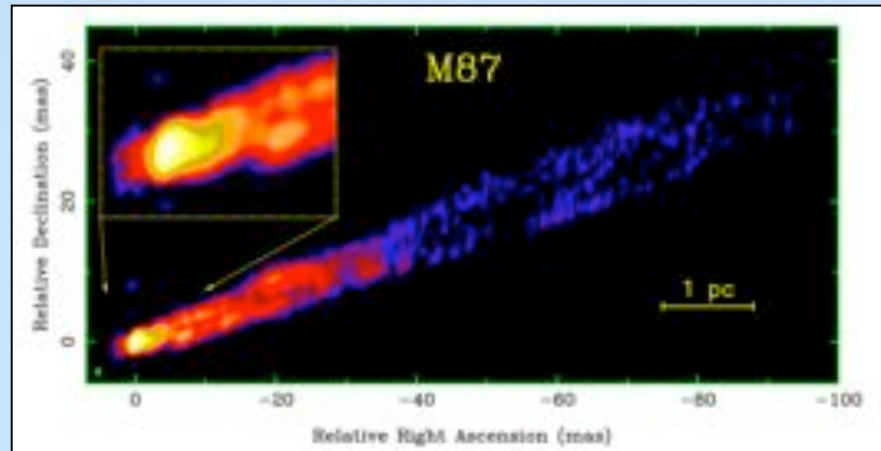
$\gamma = 10, M = 3, \eta = 10^4$
→ Relativistic spine
surrounded by a turbulent
mixing layer

$$\gamma = 10, M = 30, \eta = 10^2$$

Comparison with observations

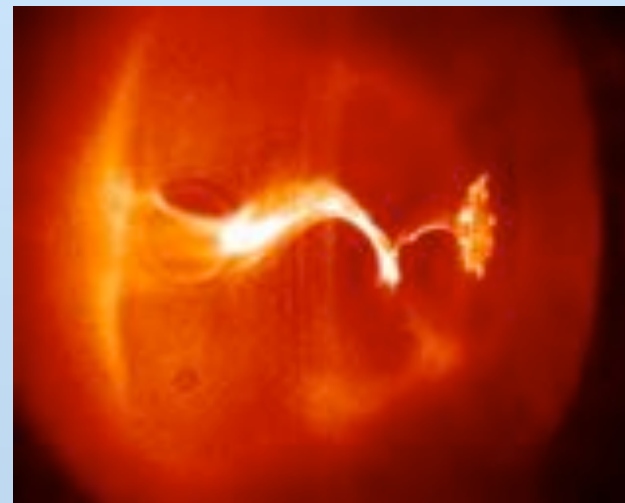
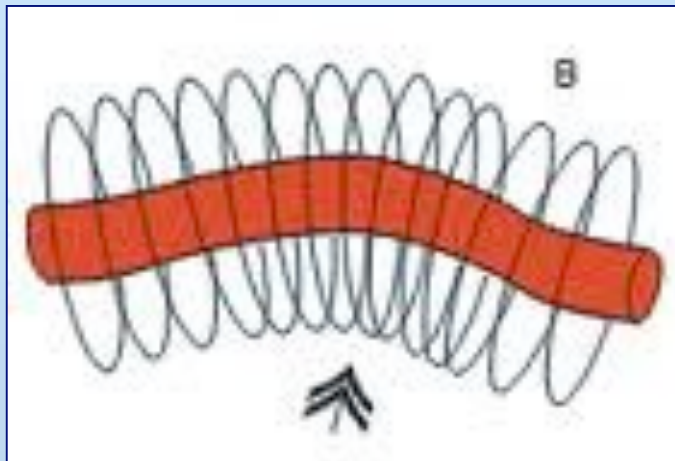
emissivity integration along the line of sight
at different projection angles

Agreement with Bridle & Laing empirical models



Intrinsic instabilities

- Current-driven kink instabilities related to a toroidal magnetic field component in current carrying jets (Bateman 1978, Appl et al. 2000, Giannios & Spruit 2006, Narayan et al. 2009)
- Stabilized by extended shears (Mizuno et al. 2007), jet expansion (Moll et al. 2008, McKinney & Blandford 2009)
- Detailed nonlinear analysis required to test instability effect on morphologies and radiation



Magnetized Jets

□ $M =$ Mach Number; $\eta = \rho_{\text{amb}}/\rho_{\text{jet}}$; $\gamma =$ Lorentz factor

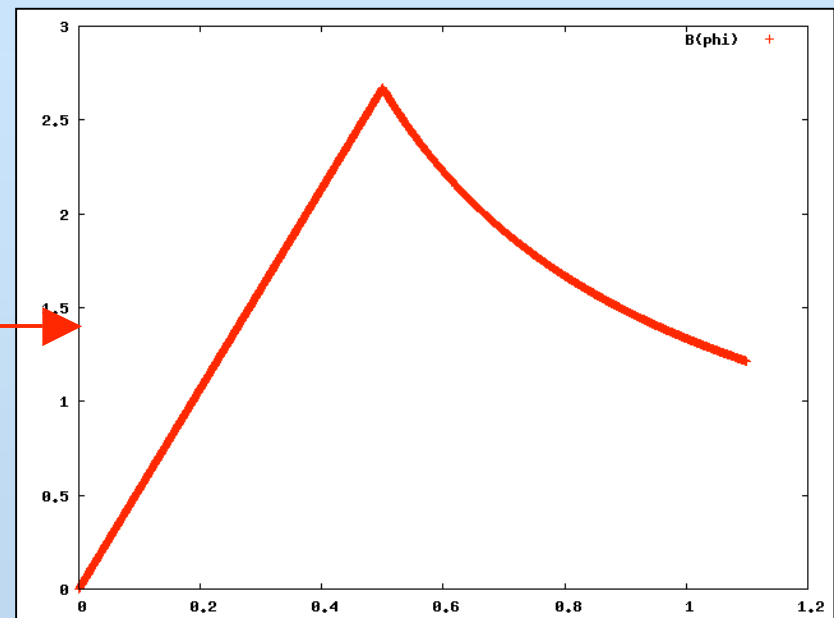
□ $\sigma =$ Magnetization $\sigma_\phi = \frac{\langle B_\phi^2 / \gamma^2 \rangle}{2\langle p_g \rangle}$ $\sigma_z = \frac{\langle B_z^2 \rangle}{2\langle p_g \rangle}$

□ Poloidal model: uniform B_z

□ Toroidal model:

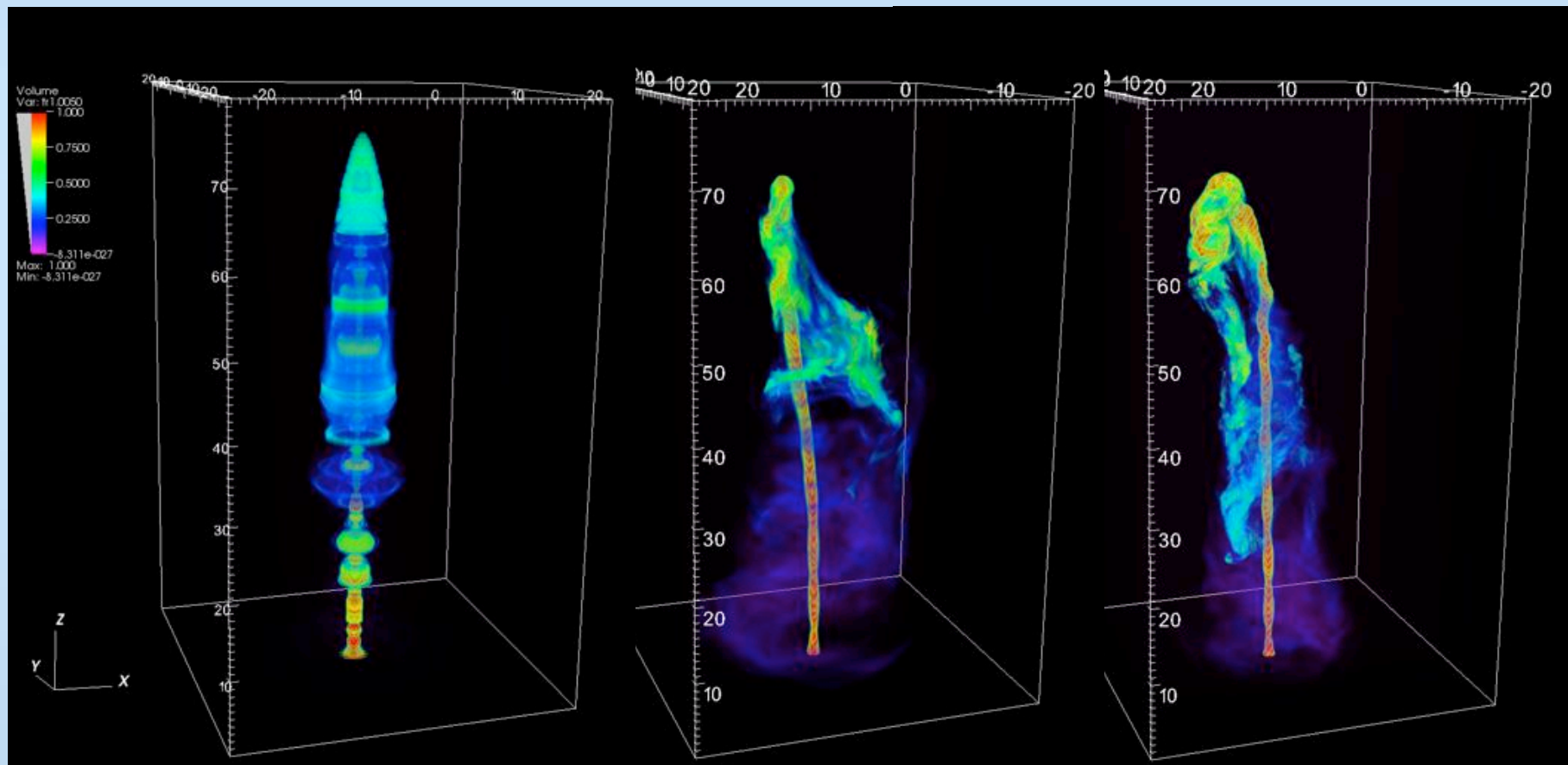
$$B_\phi = \begin{cases} B_m (r/a) & \text{for } r < a \\ B_m (a/r) & \text{for } r > a \end{cases}$$

□ $\alpha =$ Rotation $v_\phi(r) = \alpha \frac{B_\phi(r)}{B_m}$



Effects of magnetic fields

- ❑ Toroidal models shows considerable deflection
- ❑ → intrinsic 3D effect

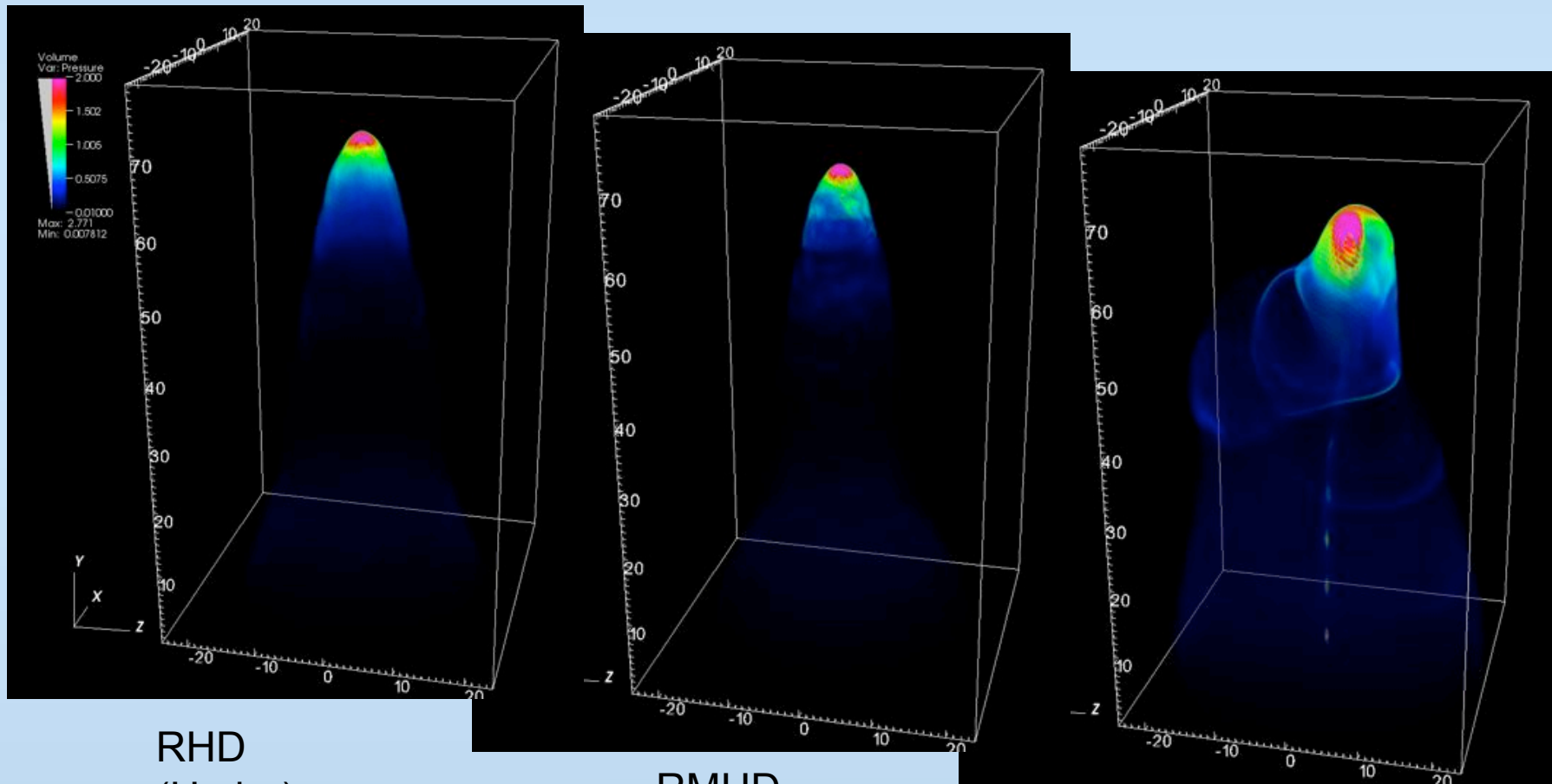


Axisym ("2.5" D)

3D LoRes

3D HiRes

Pressure distribution

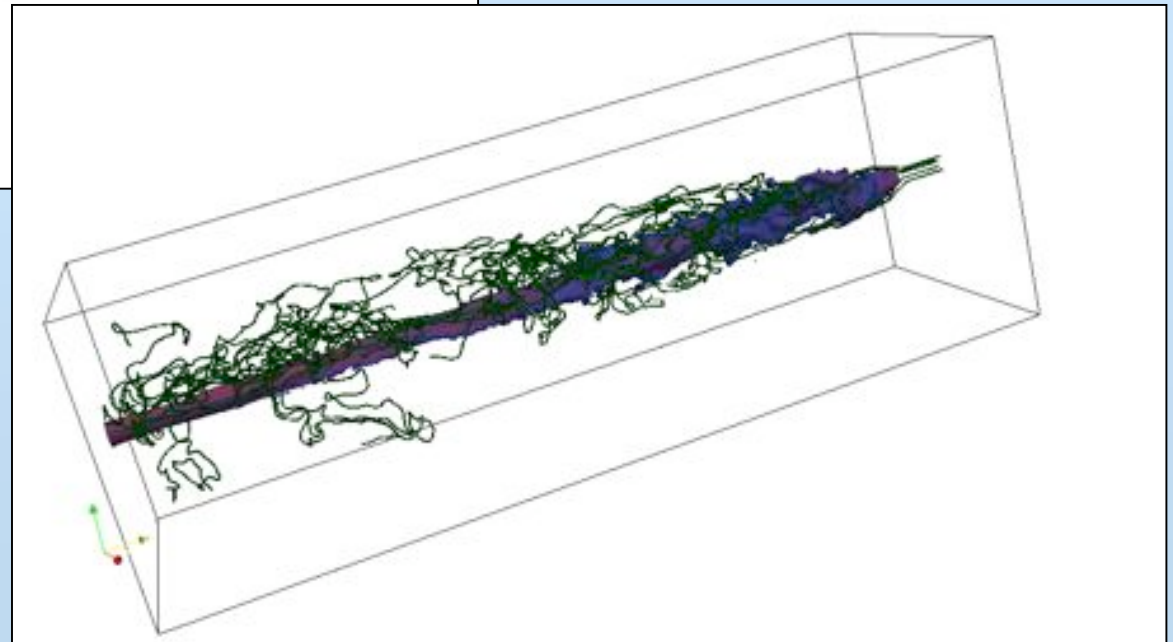
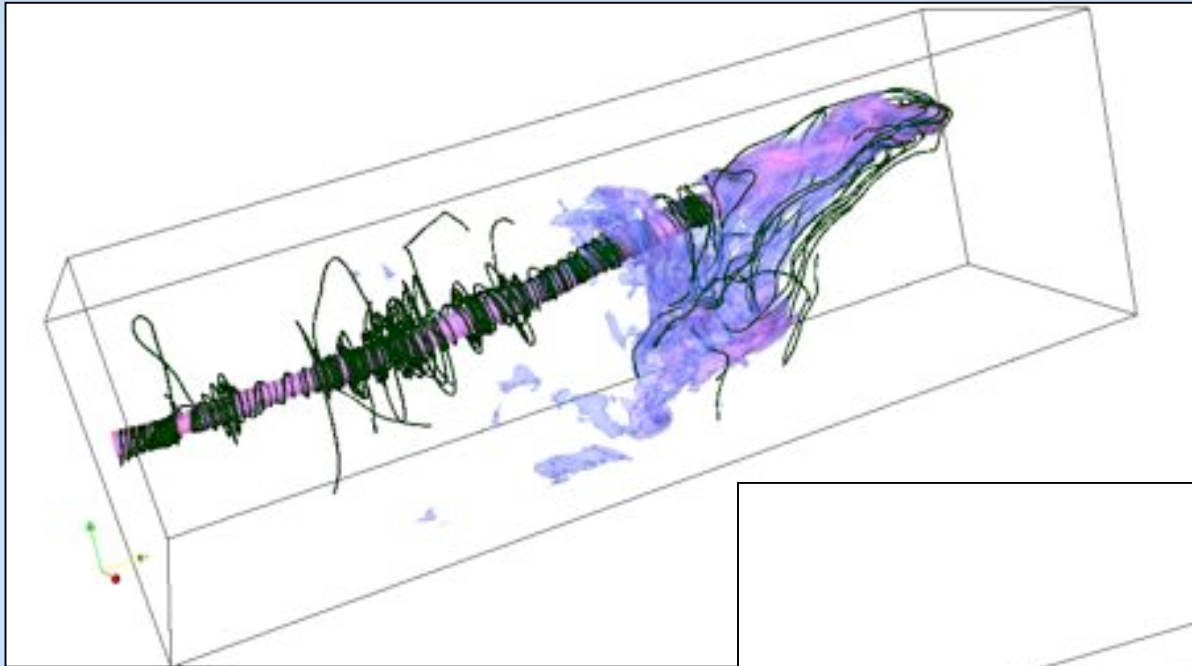


RHD
(Hydro)

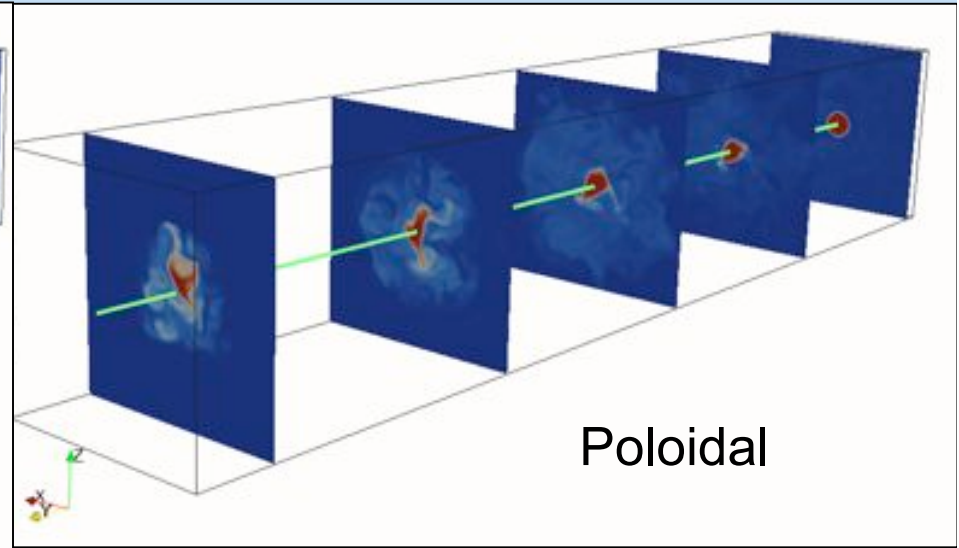
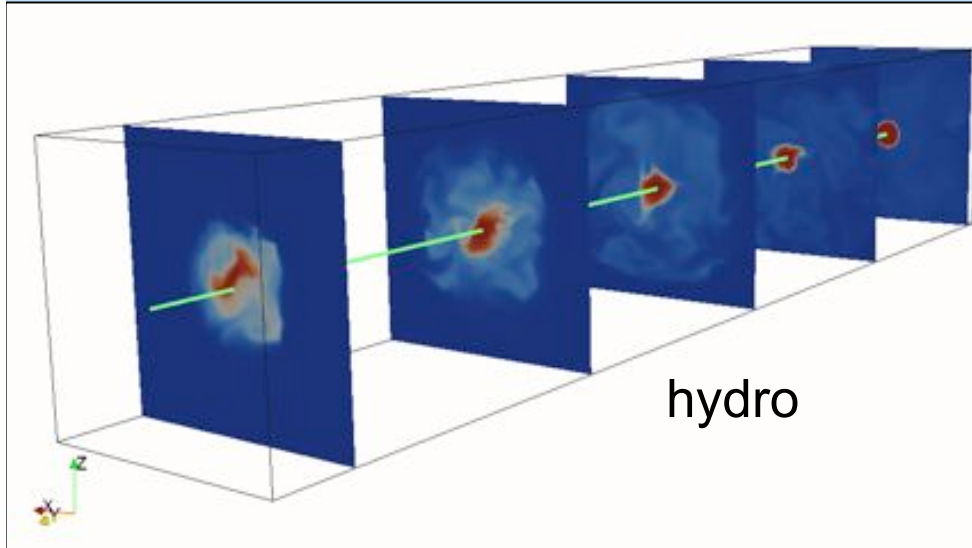
RMHD
Poloidal

RMHD
Toroidal

Magnetic Field Topology

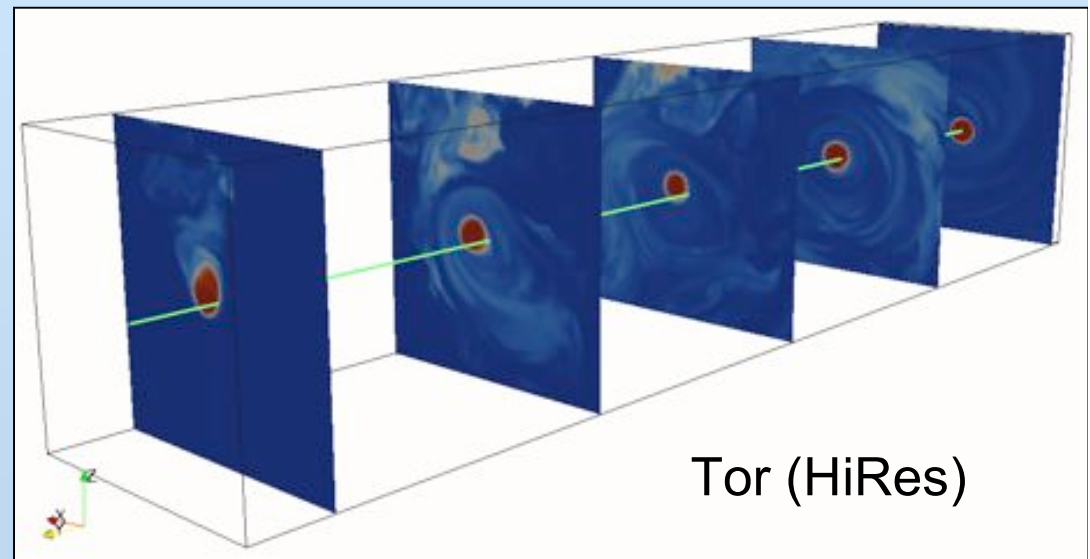


Perturbation modes



□ Hydro case and poloidal case: prevailing of short KH wavelength modes (Massaglia et al. '96, Hardee '87)

□ Toroidal case show suppression of surface modes, kink modes prevail



Kinetic to Poynting flux ratio

- Initial radial equilibrium structure:

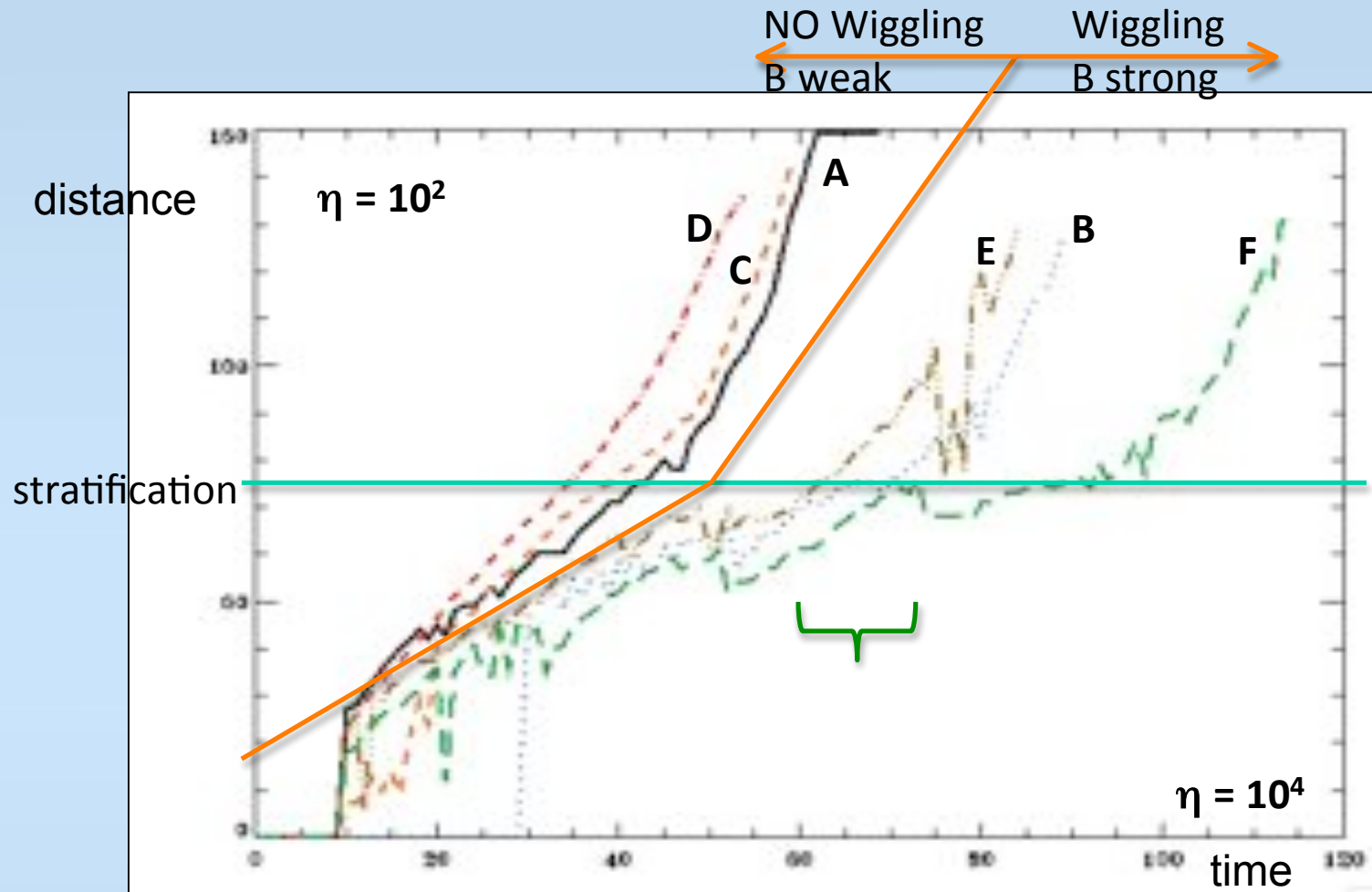
$$\frac{dp}{dr} - \frac{w\gamma^2 v_\phi^2}{r} = (\nabla \cdot \mathbf{E})\mathbf{E} + \mathbf{J} \times \mathbf{B}$$

$$E_r = -(\mathbf{v} \times \mathbf{B})_r = -(v_z B_\phi - v_\phi B_z)$$

$$(\mathbf{J} \times \mathbf{B})_r = -\left[B_z \frac{dB_z}{dr} + \frac{B_\phi}{r} \frac{d}{dr}(rB_\phi) \right]$$

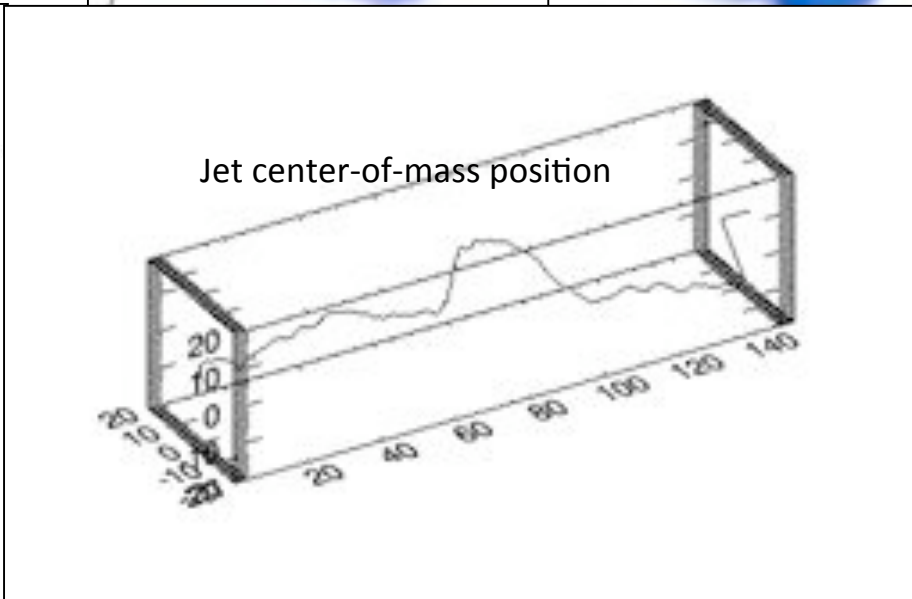
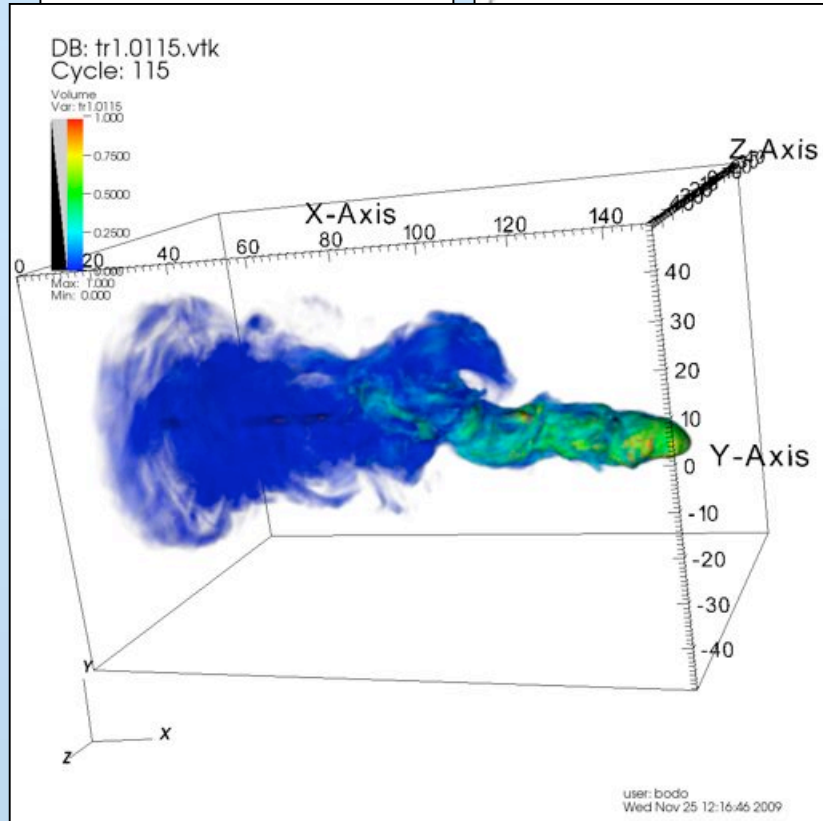
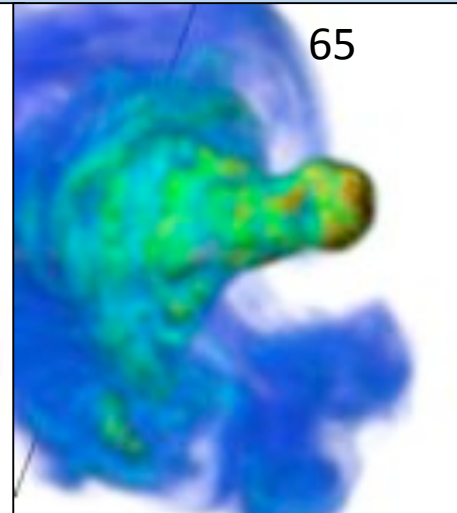
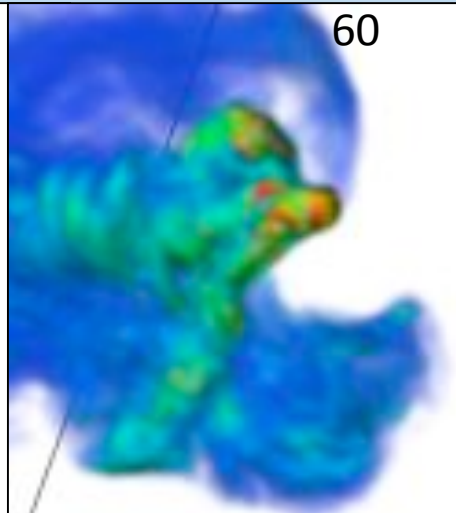
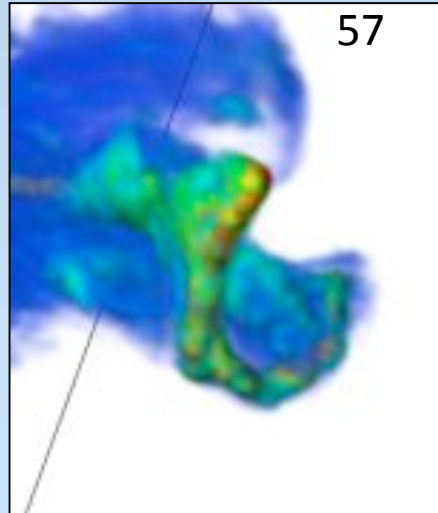
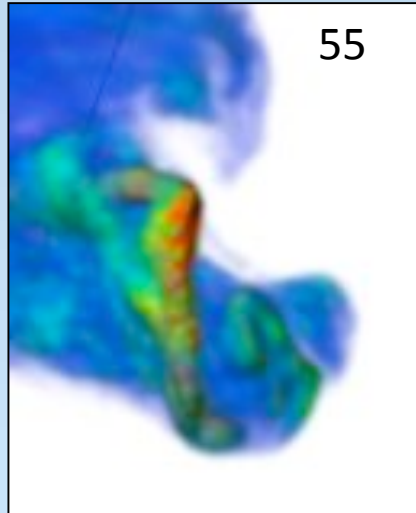
$$-\frac{dp}{dr} + \frac{w\gamma^2 v_\phi^2}{r} = \frac{1}{r^2} \frac{d}{dr} \left[\frac{(rB_\phi)^2}{2} - \frac{(rE_r)^2}{2} \right] + \frac{1}{2} \frac{dB_z^2}{dr}$$

- Relativistic jets at the inlet $\gamma = 10$
- Stratification $\eta = \rho_{\text{amb}}/\rho_{\text{jet}} = 10^4 \rightarrow 10^2$



Fluxes	A	B	C	D*	E	F
F_k/F_P	3.5	1	70	1000	3.5	1
Rotation	0	0	0	0	1	1

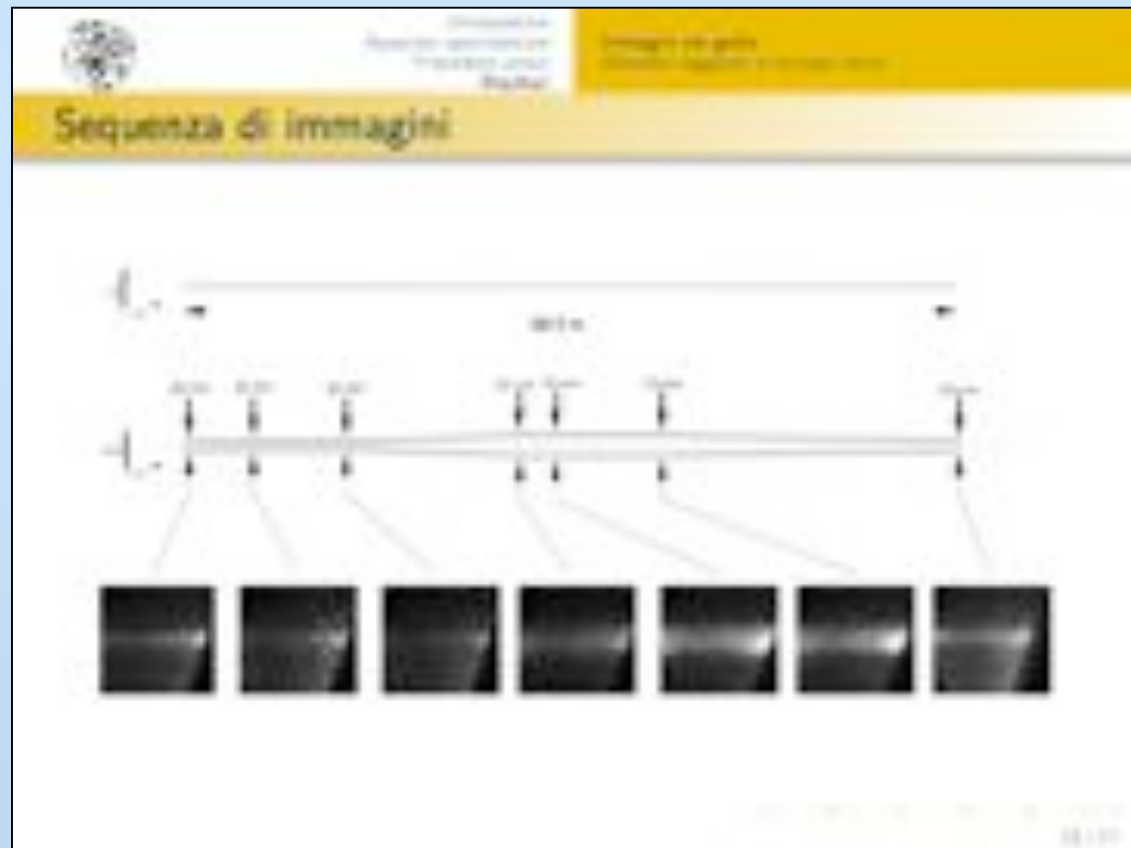
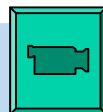
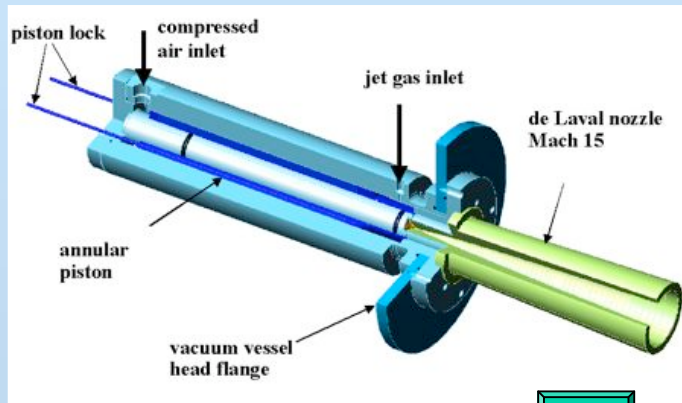
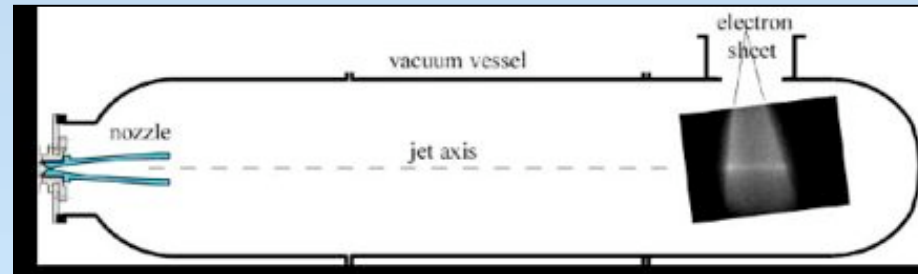
*Poloidal field



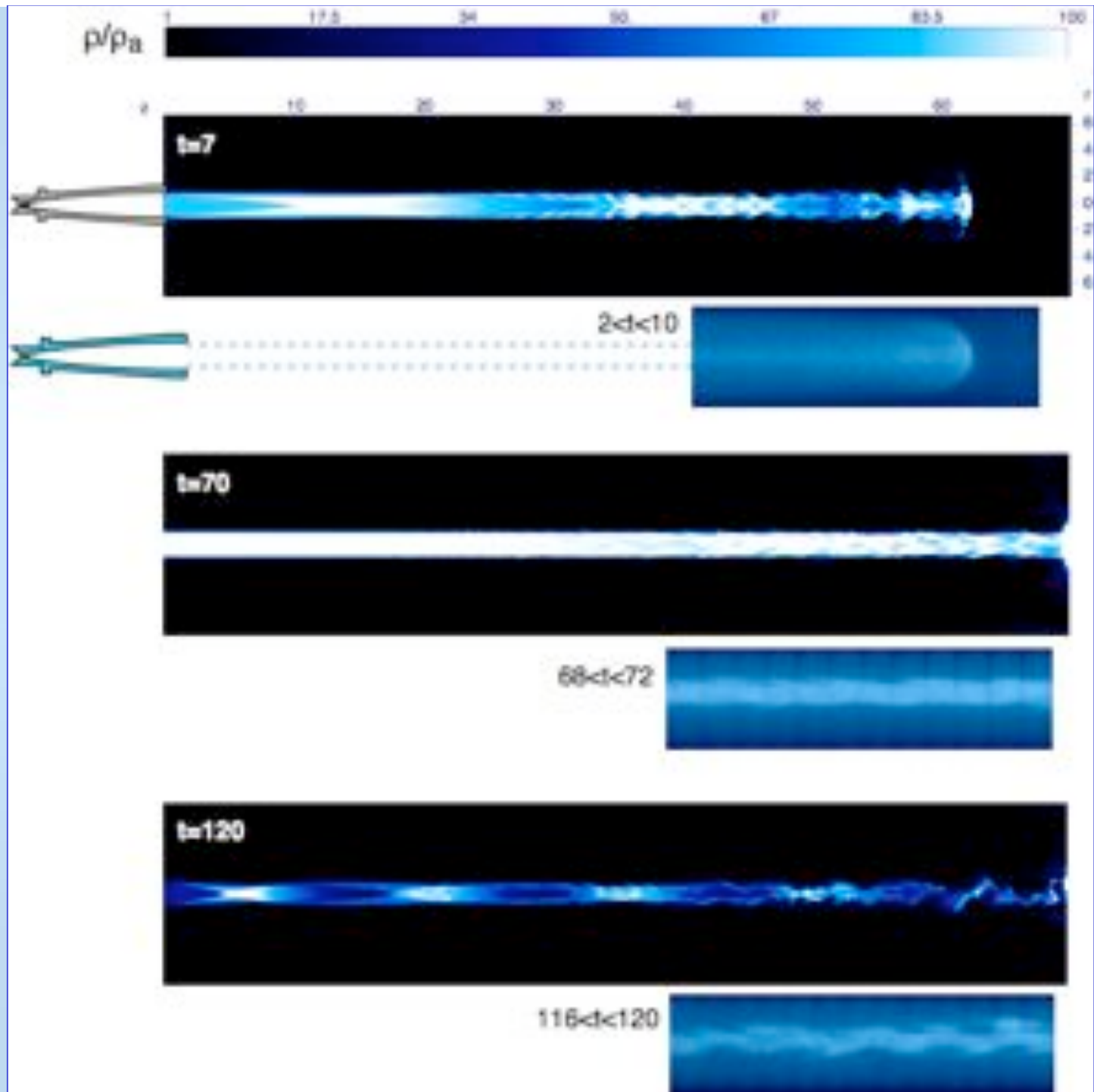
CASE F

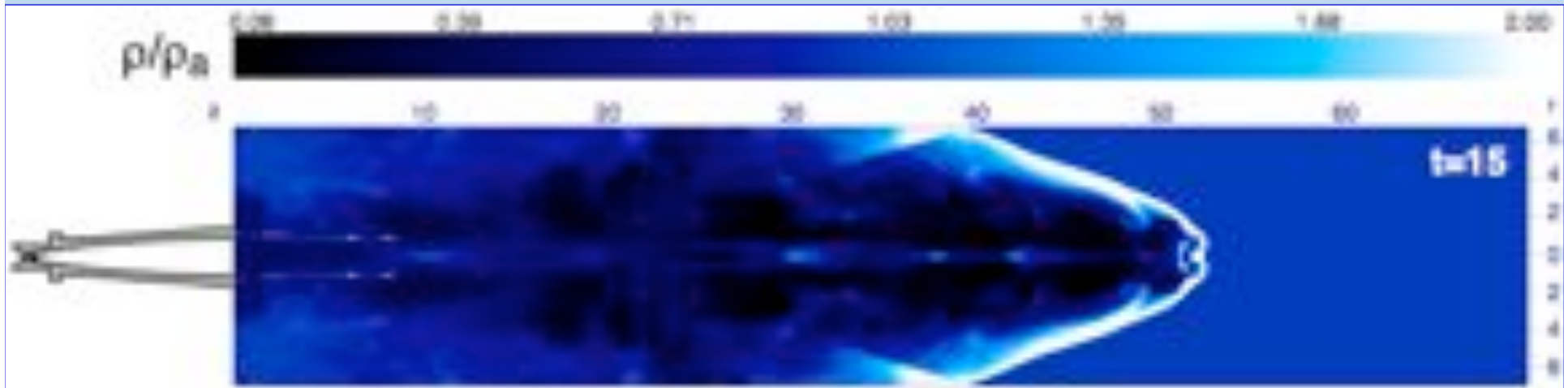
- Large Poynting fluxes produce strong kinks, the head of the flow becomes contorted
- Large kinetic fluxes avoid kinks, the heads of the jet proceeds at large velocity
- The spine of the jet is always highly relativistic on the average, shocks create intermittent structures
- When the jet encounters the low density region its structure becomes again straight and kinks disappear: hints of outflow acceleration ?

Experiment on supersonic (but not relativistic) hydro jets (Torino, Milano)



Heavy Jet





Light jet



Conclusions

- Relativistic jets show a nonlinear evolution that is different from non relativistic jets in many aspects (AGN vs star)
- Acceleration of relativistic jets in the magneto-centrifugal scheme extends beyond the fast-alfvenic point and is strictly correlated with the collimation process
- Relativistic hydro jets are subject to strong mass entrainment by shear instabilities and form naturally the spine/sheath layer structure
- Relativistic magnetized jets with strong toroidal component are subject to kink instability that may disappear when they emerge from the denser regions
- Entrainment and instabilities do not slow down the spine of the jet that remains relativistic up to the hot spot/termination shock
- The issue of jet acceleration/deceleration requires further analysis of dissipation and turbulent processes
- Particle acceleration: beyond MHD, PIC simulations
- Validation of codes on laboratory experiments is fundamental